

THESIS

TURBULENCE PARAMETERIZATIONS FOR NUMERICAL SIMULATIONS OF  
STABLY STRATIFIED ENVIRONMENTAL FLOWS

Submitted by

Zachary A. Elliott

Department of Civil and Environmental Engineering

In partial fulfillment of the requirements

For the Degree of Master of Science

Colorado State University

Fort Collins, Colorado

Spring 2011

Master's Committee:

Advisor: Subhas Karan Venayagamoorthy

Pierre Y. Julien

Lakshmi Prasad Dasi

## ABSTRACT

### TURBULENCE PARAMETERIZATIONS FOR NUMERICAL SIMULATIONS OF STABLY STRATIFIED ENVIRONMENTAL FLOWS

Almost all environmental and geophysical flows such as lakes, reservoirs, estuaries, and the atmosphere are turbulent and are also often characterized by stable density stratification. The presence of buoyancy forces due to stratification has a substantial effect on the flow development and turbulent mixing processes, influencing the distribution of pollutants and suspended matter in these flows. Mathematical and computer models can be used to simulate and produce numerical solutions to these flows, providing results that would otherwise not be feasibly attainable in a laboratory setting and that can be used for engineering prediction, design, and analysis purposes. Turbulence models use computational procedures to close the system of mean flow equations and account for the effects of turbulence and stratification through the specification of parameters that characterize the behavior of the flow. In this research, an attempt is made to assess and improve turbulence parameterizations for stably stratified environmental flows.

An important parameter describing the transfer of momentum and scalar fluxes in stratified turbulent flows is the turbulent Prandtl number  $Pr_t$ . Specifically, four different formulations of the turbulent Prandtl number  $Pr_t$  are evaluated for stably stratified flows.

All four formulations of  $Pr_t$  are strictly functions of the gradient Richardson number  $Ri$ , a parameter that provides a measure of the strength of the stratification. A zero-equation turbulence model for the turbulent viscosity  $\nu_t$  in a one-dimensional turbulent channel flow is considered to assess the behavior of the different formulations of  $Pr_t$ . Both unidirectional and oscillatory flows are considered to simulate conditions representative of practical flow problems, such as atmospheric boundary layer flows and tidally-driven estuarine flows, to quantify the behavior of each of the four formulations of  $Pr_t$ . It is discussed as to which of the models of  $Pr_t$  allow for a higher rate of turbulent mixing and which models significantly inhibit turbulent mixing in the presence of buoyancy forces resulting from fixed continuous stratification as well as fixed two-layer stratification. The basis underlying the formulation of each model in conjunction with the simulation results are used to highlight the importance of choosing an appropriate parameterization of  $Pr_t$ , given a model for  $\nu_t$  in stably stratified flows.

Other more complete and dynamic models rely on additional parameters that allow stratified turbulent flow to be modeled as a function of local turbulence quantities rather than mean global properties of the flow. This research also focuses on implementing and testing proposed changes that explicitly account for buoyancy effects in two-equation Reynolds-averaged Navier-Stokes (RANS) turbulence models. Direct numerical simulation (DNS) data of stably stratified homogeneous turbulence are used to study the parameters in two-equation RANS turbulence models such as the buoyancy parameter  $C_{\epsilon 3}$  and the turbulent Prandtl number  $Pr_t$  in the  $k$ - $\epsilon$  model. Both the gradient Richardson number  $Ri$  and the turbulent Froude number  $Fr_k$  are used as correlating parameters to characterize stratification in the  $k$ - $\epsilon$  model. It is shown that it may be more

appropriate to use  $Fr_k$  as the parameter of choice for the stratification parameter in the  $k$ - $\varepsilon$  model since it is based on the local properties of the turbulence as opposed to  $Ri$ , which is a mean property of the flow. The proposed modifications and alterations to  $C_{\varepsilon 3}$  and  $Pr_t$  as functions of  $Ri$  and  $Fr_k$  are implemented in a one-dimensional water column model called General Ocean Turbulence Model (GOTM) and used to simulate stably stratified channel flows. The results from numerical simulations using the modified versions of the  $k$ - $\varepsilon$  model are compared to stably stratified channel flow DNS data to assess their efficacy.

## **ACKNOWLEDGMENTS**

I would like to express my gratitude to each of those who in some way or another helped me to write this thesis and complete my studies for my Master of Science in Civil and Environmental Engineering degree. First, to my advisor, teacher, and mentor, Dr. Karan Venayagamoorthy, for his daily encouragement, guidance, and hard work in helping me complete my research and thesis; he truly desires his students to learn and to strive for excellence and selflessly gives of himself to that end. I am grateful to my committee members, Drs. Pierre Julien and Prasad Dasi, for all their insights and support. I also thank the rest of the academic faculty in the Civil and Environmental Engineering Department at Colorado State University who took the time to teach me and contribute to my education in any way. I would like to thank my family for their love and support in all of my endeavors; they have always been there to help me along each and every step of my life's journey. I also owe my sincere thanks to Jenika for her unending encouragement and support. Finally, nothing I have done or could ever do is possible without the abilities, blessings, and grace given to me and sustained by my Savior, Jesus Christ.

I would especially like to acknowledge the financial support I have received during the course of my studies through a graduate teaching assistantship (GTA) from the Colorado State University Department of Civil and Environmental Engineering (Head of Department – Dr. Luis Garcia) and from a graduate research assistantship (GRA)

provided through the start-up funds of Dr. S.K. Venayagamoorthy. Also, the support of the Office of Naval Research (ONR) grant N00014-10-1-0607 and scientific officers Drs. Terri Paluszkievicz and Scott Harper for my research is gratefully acknowledged.

## TABLE OF CONTENTS

Abstract .....	ii
Acknowledgments .....	v
List of Figures .....	x
Nomenclature .....	xiii
<b>CHAPTER 1: INTRODUCTION.....</b>	<b>1</b>
1.1 Introduction .....	1
1.2 Background and Motivation.....	2
1.3 Research Goals and Approach .....	4
1.4 Thesis Layout .....	5
1.5 Research Publications and Presentations .....	7
<b>CHAPTER 2: LITERATURE REVIEW OF TURBULENCE AND MODELING OF STRATIFIED ENVIRONMENTAL FLOWS.....</b>	<b>8</b>
2.1 Introduction .....	8
2.2 Governing Equations of Fluid Motion .....	10
2.3 Mean Flow Equations.....	12
2.4 Numerical Modeling Techniques .....	16
2.5 Relevant Parameters of Stratified Turbulent Flows .....	21
2.6 Characteristics of Stratified Flows .....	25
2.7 Conclusions .....	28

<b>CHAPTER 3: EVALUATION OF TURBULENT PRANDTL NUMBER PARAMETERIZATIONS USING A ZERO-EQUATION TURBULENCE MODEL</b>	<b>29</b>
3.1 Introduction .....	29
3.2 Problem Set-Up .....	30
3.3 Turbulent Prandtl Number Formulations .....	40
3.4 Results .....	45
3.5 Conclusions .....	52
<b>CHAPTER 4: DEVELOPMENT AND TESTING OF STRATIFICATION PARAMETERS IN TWO-EQUATION TURBULENCE MODELS</b>	<b>54</b>
4.1 Introduction .....	54
4.2 Problem Set-Up .....	55
4.3 Numerical Modeling .....	57
4.4 Results .....	67
4.5 Conclusions .....	80
<b>CHAPTER 5: SUMMARY AND CONCLUSIONS</b>	<b>82</b>
5.1 Summary .....	82
5.2 Conclusions .....	84
5.3 Further Work .....	85
<b>REFERENCES</b>	<b>87</b>
<b>APPENDIX A: MATLAB CODE FOR ZERO-EQUATION TURBULENCE MODEL</b>	<b>90</b>
A.1 Introduction .....	90
A.2 MATLAB Code for Zero-Equation Turbulence Model .....	91

**APPENDIX B: FORTRAN95 CODE FOR MODIFIED GOTM MODULES .....95**

B.1 Introduction .....95

B.2 buoyancy.F90 GOTM Module .....96

B.3 cmue\_vs.F90 GOTM Module.....98

B.4 cmue\_frk.F90 GOTM Module .....99

## LIST OF FIGURES

Figure 2.1.	Displacements from hydrostatic equilibrium: (a) stable; and (b) unstable density distributions .....26
Figure 2.2.	Density profiles: (a) continuous stratification density profile; and (b) two-layered stratification density profile .....26
Figure 3.1.	Schematic of the problem set-up depicting (a) the tidal velocity field; (b) a continuous stratification density profile; and (c) a two-layered stratification density profile .....34
Figure 3.2.	The turbulent Prandtl number $Pr_t$ as a function of the gradient Richardson number $Ri$ for four different models: blue dashed-dotted line, Munk and Anderson (1948); black solid line, Venayagamoorthy and Stretch (2010); purple dashed line, Kim and Mahrt (1992); red thick dashed-dotted line, Peters <i>et al.</i> (1988) .....45
Figure 3.3.	Fully developed velocity profiles and concentration profiles for the unstratified base case, (a) uni-directional flow; (b) oscillatory flow; and (c) initial concentration profile: solid line, and final concentration profile: dashed line .....46
Figure 3.4.	Concentration profiles for a passive scalar $C$ in a continuously stratified uni-directional channel flow. Subplots (a) – (c) show the initial distribution of the passive scalar plume. Final concentration profiles are shown in subplots (d) – (f) using the PGT model; subplots (g) – (i) using the MA model; subplots (j) – (l) using the VS model; and subplots (m) – (o) using the KM model, respectively. Also superimposed on subplots (d) – (o) is the final profile for the unstratified case.....48
Figure 3.5.	Concentration profiles for a passive scalar $C$ in a two-layered stratified uni-directional channel flow. Subplots (a) – (c) show the initial distribution of the passive scalar plume. Final concentration profiles are shown in subplots (d) – (f) using the PGT model; subplots (g) – (i) using the MA model; subplots (j) – (l) using the VS model; and subplots (m) – (o) using the KM model, respectively. Also superimposed on subplots (d) – (o) is the final profile for the unstratified case.....49

Figure 3.6.	Concentration profiles for a passive scalar $C$ in a continuously stratified tidally-driven channel flow. Subplots (a) – (c) show the initial distribution of the passive scalar plume. Final concentration profiles are shown in subplots (d) – (f) using the PGT model; subplots (g) – (i) using the MA model; subplots (j) – (l) using the VS model; and subplots (m) – (o) using the KM model, respectively. Also superimposed on subplots (d) – (o) is the final profile for the unstratified case .....51
Figure 3.7.	Concentration profiles for a passive scalar $C$ in a two-layered stratified tidally-driven channel flow. Subplots (a) – (c) show the initial distribution of the passive scalar plume. Final concentration profiles are shown in subplots (d) – (f) using the PGT model; subplots (g) – (i) using the MA model; subplots (j) – (l) using the VS model; and subplots (m) – (o) using the KM model, respectively. Also superimposed on subplots (d) – (o) is the final profile for the unstratified case .....52
Figure 4.1.	Density profiles: blue solid line, initial continuously stratified density profile using Dirichlet boundary conditions; black dashed line, mixed-out unstratified density profile using Neumann boundary conditions .....56
Figure 4.2.	Modular structure of GOTM.....58
Figure 4.3.	Spatial organization and indexing of the numerical grid in GOTM .....60
Figure 4.4.	Temporal organization and indexing of the numerical grid in GOTM, shown with an implicitness parameter $\sigma = 0.6$ .....61
Figure 4.5.	Distributions of (a) mean velocity $u$ ; (b) turbulent kinetic energy $k$ ; and (c) turbulent kinetic energy dissipation rate $\varepsilon$ in pressure gradient driven open-channel flow at $Re_\tau = 550$ and $Ri_\tau = 0$ : blue solid line, DNS data (García-Villalba & del Álamo 2009); black dashed line, GOTM results (standard $k$ - $\varepsilon$ model).....68
Figure 4.6.	Distributions of (a) mean velocity $u$ ; (b) turbulent kinetic energy $k$ ; and (c) turbulent kinetic energy dissipation rate $\varepsilon$ in pressure gradient driven open-channel flow at $Re_\tau = 590$ and $Ri_\tau = 0$ : blue solid line, DNS data (Moser <i>et al.</i> 1999); black dashed line, GOTM results (standard $k$ - $\varepsilon$ model) .....69
Figure 4.7.	Distributions of (a) mean velocity $u$ ; (b) density $\rho$ ; (c) turbulent kinetic energy $k$ ; and (d) turbulent kinetic energy dissipation rate $\varepsilon$ in pressure gradient driven open-channel flow at $Re_\tau = 550$ and $Ri_\tau = 60$ : blue solid line, DNS data (García-Villalba & del Álamo 2009); black dashed line, GOTM results ( $k$ - $\varepsilon$ model with constant stability functions).....71
Figure 4.8.	Distributions of (a) mean velocity $u$ ; (b) density $\rho$ ; (c) turbulent kinetic energy $k$ ; and (d) turbulent kinetic energy dissipation rate $\varepsilon$ in pressure gradient driven open-channel flow at $Re_\tau = 550$ and $Ri_\tau = 60$ : blue solid

	line, DNS data (García-Villalba & del Álamo 2009); black dashed line, GOTM results ( $k$ - $\varepsilon$ model with Munk and Anderson (1948) stability function).....	72
Figure 4.9.	Distributions of (a) mean velocity $u$ ; (b) density $\rho$ ; (c) turbulent kinetic energy $k$ ; and (d) turbulent kinetic energy dissipation rate $\varepsilon$ in pressure gradient driven open-channel flow at $Re_\tau = 550$ and $Ri_\tau = 60$ : blue solid line, DNS data (García-Villalba & del Álamo 2009); black dashed line, GOTM results ( $k$ - $\varepsilon$ model with Venayagamoorthy and Stretch (2010) stability function).....	73
Figure 4.10.	The turbulent Prandtl number $Pr_t$ as a function of the turbulent Froude number $Fr_k$ as defined in equation (4.16) .....	77
Figure 4.11.	Distributions of (a) mean velocity $u$ ; (b) density $\rho$ ; (c) turbulent kinetic energy $k$ ; and (d) turbulent kinetic energy dissipation rate $\varepsilon$ in pressure gradient driven open-channel flow at $Re_\tau = 550$ and $Ri_\tau = 60$ : blue solid line, DNS data (García-Villalba & del Álamo 2009); black dashed line, GOTM results ( $k$ - $\varepsilon$ model with $Pr_t = f(Fr_k)$ and $C_{\varepsilon 3} = 1.44$ ).....	78
Figure 4.12.	The buoyancy parameter $C_{\varepsilon 3}$ as a function of the turbulent Froude number $Fr_k$ as defined in equation (4.17) .....	79
Figure 4.13.	Distributions of (a) mean velocity $u$ ; (b) density $\rho$ ; (c) turbulent kinetic energy $k$ ; and (d) turbulent kinetic energy dissipation rate $\varepsilon$ in pressure gradient driven open-channel flow at $Re_\tau = 550$ and $Ri_\tau = 60$ : blue solid line, DNS data (García-Villalba & del Álamo 2009); black dashed line, GOTM results ( $k$ - $\varepsilon$ model with $Pr_t = f(Fr_k)$ and $C_{\varepsilon 3} = f(Fr_k)$ ).....	80

## NOMENCLATURE

The notation used is given here in the following order: upper-case Roman, lower-case Roman, upper-case Greek, lower-case Greek, subscripts and superscripts, and abbreviations.

### Upper-case Roman

$B$	buoyancy flux or buoyancy production rate of turbulent kinetic energy
$C$	passive scalar concentration
$C_D$	drag coefficient
$C_{\varepsilon 1}$	constant in the model equation for $\varepsilon$
$C_{\varepsilon 2}$	constant in the model equation for $\varepsilon$
$C_{\varepsilon 3}$	buoyancy parameter in the model equation for $\varepsilon$
$C_{\varepsilon 3,0}$	maximum value of $C_{\varepsilon 3}$
$C_{\mu}$	turbulent-viscosity constant in the $k$ - $\varepsilon$ model
$D_k$	diffusion of turbulent kinetic energy
$D_{\varepsilon}$	diffusion transport term in the model equation for $\varepsilon$
$Fr$	Froude number
$Fr'$	internal Froude number
$Fr_k$	turbulent Froude number
$H$	total flow depth
$L$	characteristic lengthscale of the flow or turbulence lengthscale
$L_O$	buoyancy or Ozmidov lengthscale
$M_2$	Semidiurnal tidal constituent
$N$	Brunt-Väisälä or buoyancy frequency
$N_i$	number of grid layers
$P$	production rate of turbulent kinetic energy due to shear
$Pr$	Prandtl number
$Pr_t$	turbulent Prandtl number
$Pr_{t0}$	neutral (unstratified) value of the turbulent Prandtl number
$R_{f\infty}$	asymptotic value of the flux Richardson number

$Re$	Reynolds number
$Re_\tau$	friction Reynolds number
$Ri$	gradient Richardson number
$Ri_\tau$	friction Richardson number
$S$	mean strain rate tensor or mean velocity gradient
$Sc$	Schmidt number
$T$	tidal period
$T_L$	mechanical or turbulence timescale
$T_\rho$	scalar timescale
$U$	characteristic velocity scale of the flow
$U_{\max}$	maximum flow velocity

### Lower-case Roman

$g$	gravitational acceleration
$h_i$	grid layer height or thickness
$k$	turbulent kinetic energy
$p$	pressure
$\bar{p}$	mean pressure
$t$	time
$u$	fluid velocity
$u'$	fluctuating fluid velocity
$\bar{u}$	mean fluid velocity
$u_1$	fluid velocity at the first grid point from the lower channel boundary
$u_\tau$	shear or friction velocity
$\overline{u'_i u'_j}$	Reynolds stress tensor
$w'$	$z$ -component of fluctuating velocity
$x$	cartesian coordinate
$y$	cartesian coordinate
$z$	cartesian coordinate
$z_{pyc}$	mid-depth of a pycnocline

### Upper-case Greek

$\Gamma$	molecular heat or scalar diffusivity
$\Gamma_\infty$	mixing efficiency
$\Gamma_t$	turbulent diffusivity or scalar eddy diffusivity
$\Gamma_{t \text{mod}}$	modified scalar eddy diffusivity
$\Delta$	finite grid width, spacing, or difference
$T$	time level

### Lower-case Greek

$\alpha$	empirical constant in the Munk and Anderson (1948) model for $\nu_t$
$\alpha_\rho$	empirical constant in the Munk and Anderson (1948) model for $\Gamma_t$
$\beta$	empirical constant in the Munk and Anderson (1948) model for $\nu_t$
$\beta_\rho$	empirical constant in the Munk and Anderson (1948) model for $\Gamma_t$
$\gamma$	$(1/2)(T_t/T_\rho)$
$\delta_{ij}$	Kronecker delta
$\varepsilon$	rate of dissipation of turbulent kinetic energy
$\zeta$	empirical constant in the model equation for $Pr_t = f(Fr_k)$
$\eta$	free surface elevation
$\theta$	implicitness parameter used in the $\theta$ -method
$\kappa$	von Karman constant
$\nu$	molecular momentum diffusivity or kinematic viscosity
$\nu_t$	turbulent viscosity or kinematic eddy viscosity
$\nu_{t \text{mod}}$	modified eddy viscosity
$\nu_{t \text{mod},\text{pyc}}$	value of $\nu_{t \text{mod}}$ computed at the mid-depth of a pycnocline
$\rho$	density
$\rho'$	fluctuating density or density variation
$\bar{\rho}$	mean density
$\rho_0$	background or reference mean density
$\sigma$	implicitness parameter used in GOTM
$\sigma_k$	turbulent Prandtl number for kinetic energy
$\sigma_\varepsilon$	turbulent Prandtl number for dissipation
$\phi$	conserved passive scalar
$\bar{\phi}$	mean conserved passive scalar
$\overline{\phi'u'_i}$	Scalar flux
$\psi$	empirical constant in the model equation for $Pr_t = f(Fr_k)$
$\omega$	specific dissipation

### Superscripts and Subscripts

$i$	spatial grid or tensor index (1, 2, or 3)
$j$	tensor index (1, 2, or 3)
$n$	temporal grid index

### Abbreviations

APS	American Physical Society
ASCE	American Society of Civil Engineers
CFD	computational fluid dynamics

DFD	Division of Fluid Dynamics
DNS	direct numerical simulation
GOTM	General Ocean Turbulence Model
KM	Kim and Mahrt (1992)
LES	large-eddy simulation
MA	Munk and Anderson (1948)
PDE	partial differential equation
PGT	Peters <i>et al.</i> (1988)
RANS	Reynolds-averaged Navier-Stokes
VS	Venayagamoorthy and Stretch (2010)

# CHAPTER 1

## INTRODUCTION

### 1.1 Introduction

Stable density stratification is a common feature in turbulent environmental flows such as rivers, lakes, reservoirs, estuaries, oceans, and the atmospheric boundary layer. Stable stratification is characterized by a density gradient in which the density of the fluid increases with depth in a river, lake, or ocean or decreases with altitude in the atmosphere. This stable stratification can occur continually or can be marked by a denser fluid layer (e.g. salt water from the ocean) flowing beneath a less dense fluid layer (e.g. fresh water from a river) separated by a distinct interface. The interface of these two layers forms a sharp density gradient within the flow, often referred to as a pycnocline or thermocline. In either case, stable stratification tends to suppress turbulence; the buoyancy flux term in the governing equation for the turbulent kinetic energy of a flow acts as an energy sink in the presence of stable stratification to inhibit vertical mixing and dispersion from the turbulence generated from shear stress at the bottom boundary. As a result, turbulent properties of the flow that describe the vertical mixing and diffusion of momentum and scalars called the eddy viscosity and scalar eddy diffusivity respectively are significantly affected, especially away from boundaries where turbulence is

generated. Essentially, stable stratification and turbulence compete with one another to determine the rate and efficiency of vertical turbulent mixing in a stably stratified turbulent flow. Fundamental research in this field is aimed at understanding this intricate coupling between stratification and turbulence with the overarching goal of developing improved models that capture this two-way coupling for use in computational fluid dynamics (CFD) simulations.

## **1.2 Background and Motivation**

Predicting the vertical mixing and dispersion of a passive scalar, such as the concentration of a pollutant released at some depth within a stably stratified environmental flow, can be achieved by numerically solving the equations that govern the motion and properties of the flow. The equations that govern the behavior of a fluid are the well-known Navier-Stokes equations for conservation of momentum and the continuity equation for conservation of mass. However, it is not feasible in most cases to solve the highly nonlinear set of Navier-Stokes equations in their full form using direct numerical simulations (DNS) or large-eddy simulations (LES) due mainly to computational and geometrical constraints. A practical approach commonly used in engineering to obtain approximate (statistical) solutions to the Navier-Stokes equations is to use Reynolds decomposition to cast them in terms of time-averaged variables by splitting each instantaneous variable into a mean component and a fluctuating component. This averaging process yields the so called Reynolds-averaged Navier-Stokes (RANS) equations and results in six additional terms called the Reynolds stresses in the

averaged momentum equations and a turbulent scalar flux term in the scalar (density) transport equation. These turbulent flux terms give rise to what is commonly known as the closure problem in turbulent flows and hence necessitate the need for additional equations/models to close the system of equations (i.e. have enough equations to solve for each of the unknowns) in order to obtain solutions.

There are different computational methods for closing the RANS system of mean flow equations known as turbulence models, many of which rely on the turbulent Prandtl number  $Pr_t = \nu_t/\Gamma_t$  to link the scalar eddy diffusivity  $\Gamma_t$  and the eddy viscosity  $\nu_t$  (Venayagamoorthy & Stretch 2010). Turbulence models may vary in complexity and completeness; for example a more complete method, which is more computationally expensive, is to solve six transport equations for each of the Reynolds stresses. However, a common approach is to use the Boussinesq turbulent-viscosity hypothesis to model the Reynolds stresses  $\overline{u'_i u'_j}$  as a linear function of the mean strain rate tensor  $S$  multiplied by  $\nu_t$ . Again, there are different approaches to modeling  $\nu_t$  ranging from more complete two-equation turbulence models to simplified zero-equation algebraic models. Two-equation turbulence models such as the  $k$ - $\varepsilon$  model describe  $\nu_t$  as a function of the turbulent kinetic energy  $k$  and the turbulent kinetic energy dissipation rate  $\varepsilon$ , which are in turn given by two partial differential equations (PDEs) that must be solved within the framework of the RANS equations. Zero-equation models are the simplest turbulence models that use algebraic expressions for the eddy viscosity and hence do not require the solution of any additional PDEs (Chen & Jaw 1998, Ferziger & Peric 2002). They are therefore easy to implement and can often yield accurate and insightful results for certain (simple) types of turbulent flows.

Numerous turbulence models have been proposed and used to model and simulate a broad range of turbulent flows. However, there still exists a great deal of potential to improve upon the existing limitations and overall effectiveness of current RANS models. For stratified turbulent flows, a general and comprehensive formulation of the many of the parameters that describe and define turbulence models, including  $Pr_t$  and  $\nu_t$ , has yet to be achieved and is thus an ongoing research task. By defining these key parameters in terms of the correct fundamental variables and properties that govern fluid dynamics and only through comparison to physical and simulation data of stratified turbulence can better and more robust turbulence models be established.

### **1.3 Research Goals and Approach**

The goals of this research are to investigate the effects of stable stratification on parameters that describe the vertical mixing and diffusion of momentum and scalars, including  $Pr_t$  and the buoyancy parameter  $C_{\epsilon 3}$  in the standard  $k$ - $\epsilon$  model, and to clarify the definition of these parameters using numerical simulations of the RANS equations. These parameters, being adjusted to account for the effects of stable stratification and buoyant forces, can be defined as either constants or functions of the strength of stratification and mean properties of the flow and/or local properties of the turbulence. The results of the numerical simulations can then be validated by comparison to DNS data to determine the efficacy of the parameter formulations and the standard  $k$ - $\epsilon$  model in itself to handle stratified turbulent flows.

The numerical simulations are carried out by using both a simple zero-equation turbulence model and the two-equation standard  $k-\varepsilon$  turbulence model. The zero-equation turbulence model is coded in MATLAB and applied to a one-dimensional channel flow problem to test different formulations of  $Pr_t$ . The results of the vertical diffusion of a passive scalar are compared to one another (in a relative sense) to analyze their behavior under stably stratified conditions. Two different types of flow, uni-directional and oscillatory channel flow, are considered in this model to also test its applicability and robustness to different geophysical flow scenarios. A more comprehensive two-equation model is also used to test turbulence and stratification parameters, including  $Pr_t$ , used in these models. The standard  $k-\varepsilon$  model, present within the framework of a developed one-dimensional water column turbulence model called General Ocean Turbulence Model (GOTM), is employed to simulate one-dimensional, fully developed channel flow in order to test model parameters through validation and comparison to DNS data for stably stratified channel flow.

## **1.4 Thesis Layout**

The next four chapters of this thesis present the technical content of this research, including background information, methodology, results, discussion, and conclusions. The appendices include the computer codes that were developed and/or modified for this study to simulate numerical solutions of stably stratified turbulent flows.

Chapter two provides background information gathered from a review of published literature on turbulence and modeling of stably stratified environmental flows.

Specifically, it highlights some of the fundamentals of fluid dynamics and turbulence, the challenges associated with modeling stratified turbulent flows, and methods in which these types of flows are modeled. In addition, it summarizes the basic theory and knowledge, including definitions, governing equations, and methodology, included in this research.

Chapter three presents a study of the effect of stable stratification on  $Pr_t$  using a zero-equation turbulence model for  $\nu_t$  in a one-dimensional turbulent channel flow. The behavior of four different formulations of  $Pr_t$  for four different open-channel flow cases are evaluated with regard to the predicted rate of vertical turbulent mixing of a passive scalar in the presence of buoyancy forces resulting from the imposed density stratification. The results of this study highlight the importance of and provide a basis for choosing an appropriate parameterization of  $Pr_t$  given a model for  $\nu_t$  in stably stratified flows.

Chapter four is dedicated to the study of implementing and testing modifications to parameter formulations that explicitly account for buoyancy effects in two-equation RANS turbulence models, namely  $Pr_t$  and  $C_{\epsilon 3}$ . The modifications are applied to the one-dimensional water column turbulence model, General Ocean Turbulence Model (GOTM), and used to simulate stably stratified channel flows. Using the standard  $k-\epsilon$  model available in GOTM, the results of these simulations are compared to DNS data for stably stratified turbulent channel flows to assess the efficacy of the modified parameter formulations for use in two-equation RANS turbulence models.

Chapter five is a summary of the research done and main conclusions found in these studies. It highlights the contributions made to research of stably stratified turbulent

flows, both as an extension of the work of others and as new findings and ideas. Finally, it gives suggestions for further work to be completed as an extension of this study.

Appendix A contains the MATLAB code developed to simulate and compute results for the zero-equation turbulence model study in chapter three. Appendix B provides the FORTRAN95 code for each of the GOTM modules or subroutines that were modified to simulate and compute results using the  $k$ - $\varepsilon$  model pertaining to the study in chapter four.

## **1.5 Research Publications and Presentations**

This thesis contains substantial portions of a peer-reviewed journal publication entitled “Evaluation of turbulent Prandtl (Schmidt) number parameterizations for stably stratified environmental flows” by Z.A. Elliott and S.K. Venayagamoorthy in the journal *Dynamics of Atmospheres and Oceans*. A talk entitled “Evaluation of turbulent Prandtl (Schmidt) number parameterizations for stably stratified turbulent flows” was also presented at the 63<sup>rd</sup> Annual Meeting of the American Physical Society (APS) – Division of Fluid Dynamics (DFD) in Long Beach, California, November 21 – 23, 2010.

A portion of this thesis on the two-equation turbulence model study has also been accepted in paper and oral presentation form to the Hydraulics and Waterways Track at the 2011 World Environmental & Water Resources Congress of the American Society of Civil Engineers (ASCE). Further extensions of this work are in preparation for submission as a peer-reviewed journal publication in *Physics of Fluids*.

## **CHAPTER 2**

# **LITERATURE REVIEW OF TURBULENCE AND MODELING OF STRATIFIED ENVIRONMENTAL FLOWS**

### **2.1 Introduction**

Turbulence occurs every day in most practical flows of engineering relevance. An essential feature of turbulent flows is that the fluid velocity field varies in both space and time. Furthermore, this variation is always irregular and non-uniform, which makes it hard to predict and model. Turbulence enhances the rates of mixing of momentum, heat, and other variables of interest, making the application of turbulence modeling and understanding broad and useful. The majority of environmental or geophysical flows (i.e. oceans, lakes, estuaries, and the atmosphere) are also influenced substantially by density stratification. These stratified flows have a wide range of engineering applications ranging from pollutant mixing and dispersion in an estuary to reservoir hydraulics to weather prediction and forecasting. Stratified flows are marked by a density gradient with respect to the depth of the flow, causing buoyant forces that can significantly influence the flow patterns and the mixing of both momentum and scalars (Rodi 1987). In flows that are both turbulent and stratified, the interaction between the buoyant forces and the turbulence are dynamically coupled and influence one another. This interaction presents a

great modeling challenge for applications such as those discussed above and hence calls for a more in-depth and fundamental understanding of stratified turbulence.

Modeling stratified and unstratified turbulent fluid flows still remains one of the most difficult challenges in all of fluid mechanics due to the nature of turbulence, which is described by the Navier-Stokes equations. For example, the instantaneous turbulent velocity field is three-dimensional with spatial-temporal variations over a wide range of timescales and lengthscales. The largest scales of turbulent motion in the flow are not universal as they depend on the boundaries and geometry of a given flow problem. The nonlinear convective term in the governing Navier-Stokes equations is difficult to solve for and model. Even more difficult is the pressure gradient term due to its non-local nature. Turbulence is marked by characteristics such as randomness and nonlinearity and a unique analytic solution the Navier-Stokes equations that describe the motion of fluid substances has yet to be obtained (Pope 2000).

These are just a few of the specific challenges that are faced in describing, solving, and modeling stratified and unstratified turbulent flows. However, recent progress has been made in the field of turbulence, both in theory and observations, and a wide range of mathematical and computational techniques have been developed for practical flow problems to model turbulence (Kundu 1990). Computational fluid dynamics (CFD), as an example, is a branch of fluid engineering, mathematics, and computer science that uses numerical methods and algorithms to discretize and solve the governing equations of fluid motion using computers.

## 2.2 Governing Equations of Fluid Motion

The Navier-Stokes equations that govern the motion of a fluid are a set of nonlinear partial differential equations named after Claude Louis Marie Henri Navier and George Gabriel Stokes, who worked independently to derive them over 150 years ago (Anderson 1998). These equations that describe the conservation of momentum for a Newtonian fluid in accordance with Newton's second law can be written using tensor notation as

$$\frac{\partial u_i}{\partial t} + \frac{\partial}{\partial x_j} (u_i u_j) = -\frac{1}{\rho} \frac{\partial p}{\partial x_i} + \nu \frac{\partial^2 u_i}{\partial x_j \partial x_j} - g \delta_{i3}. \quad (2.1)$$

The terms on the left-hand side of equation (2.1) represent the total or material derivative of the velocity field  $u_i$ , consisting of an unsteady local acceleration term plus a nonlinear convective acceleration term associated with the change in velocity with respect to position, respectively. The terms on the right-hand side of equation (2.1) account for the forces acting on the fluid. The first term on the right-hand side corresponds to the pressure forces; the second term describes the viscous forces arising from shear stress, and the third term represents a body force due to gravity. In addition to the Navier-Stokes equations for conservation of momentum, the continuity equation describing the conservation of mass also governs fluid flow and can be written as

$$\frac{\partial \rho}{\partial t} + \frac{\partial}{\partial x_i} (\rho u_i) = 0. \quad (2.2)$$

According to the Boussinesq approximation for an incompressible flow, when density variations of the fluid  $\rho'$  are small compared to the background or reference mean density  $\rho_0$ ,  $\rho'$  generates only a small correction to the inertia terms on the left-hand side of equation (2.1) and can be neglected. However, in the gravity (or buoyancy) term on the right-hand side of equation (2.1) where the density  $\rho$  is multiplied by gravitational acceleration  $g$ , the effect of  $\rho'$  is substantial and cannot be neglected (Kundu 1990). Thus, assuming the Boussinesq approximation holds, equation (2.1) can be simplified and rewritten as

$$\frac{\partial u_i}{\partial t} + \frac{\partial}{\partial x_j} (u_i u_j) = -\frac{1}{\rho_0} \frac{\partial p}{\partial x_i} + \nu \frac{\partial^2 u_i}{\partial x_j \partial x_j} - \frac{\rho}{\rho_0} g \delta_{i3}. \quad (2.3)$$

Applying the Boussinesq approximation to the continuity equation (2.2) yields the incompressible form of the continuity equation for conservation of mass, which can be written as

$$\frac{\partial u_i}{\partial x_i} = 0. \quad (2.4)$$

In addition to the mass of the fluid, passive scalars in a flow are also conserved and governed by the scalar conservation equation. Scalar values that are passive are assumed to have no effect on the material properties of the flow itself such as  $\rho$ , the molecular kinematic viscosity  $\nu$ , and the molecular diffusivity  $\Gamma$  and therefore do not influence the flow field  $u_i$  (Pope 2000). For a passive scalar  $\phi$  transported by a constant-

property flow without a source or sink term, the advection-diffusion equation governing the motion of  $\phi$  can be written as

$$\frac{\partial \phi}{\partial t} + \frac{\partial}{\partial x_i} (\phi u_i) = \Gamma \frac{\partial^2 \phi}{\partial x_i \partial x_i}, \quad (2.5)$$

where  $\Gamma$  is the molecular diffusivity of  $\phi$ . In the case of an active scalar, such as  $\rho$ , equation (2.5) describing the conservation of  $\rho$  and equation (2.1) governing the motion of the flow cannot be considered independent of one another. The equations are inherently coupled dynamically (this is further addressed in section six of this chapter), which makes the solution of density stratified flows intriguing and challenging in addition to the already complex nature of the Navier-Stokes equations for unstratified turbulent flow.

### 2.3 Mean Flow Equations

Given that the equations describing fluid flow are known, where then does the challenge lie (besides solving complex, nonlinear, and sometimes coupled differential equations)? The challenge in modeling and predicting fluid flow based on the governing equations comes from the vast amount of information contained in the velocity field solution of the equations (i.e. a large range of scales for high  $Re$  flows). This makes a direct computation, or direct numerical simulation (DNS), impractical and virtually impossible for moderate to highly turbulent flows. Often times when considering turbulent geophysical and engineering flows, the solution of the full set of the governing

equations yielding the exact and instantaneous velocity field of the flow is not entirely necessary and/or feasible. With that said, the goal is to describe turbulent flows not in terms of the instantaneous velocity field, but rather with some statistics (e.g. the mean velocity field) that vary smoothly (if at all) in space and time. This is a tractable approach to solving the Navier-Stokes equations and is much less costly and daunting (Pope 2000).

In 1884 Osborne Reynolds first derived the governing equations describing the mean turbulent velocity field from the Navier-Stokes equations, a set of time-averaged equations of motion for fluid flow that would come to be known as the Reynolds-averaged Navier-Stokes (RANS) equations. They are derived by first noting that at any point in time, the instantaneous turbulent velocity  $u_i$  can be expressed as in terms of its mean  $\bar{u}_i$  and its deviation from the mean or fluctuation  $u'_i$ . This decomposition of the turbulent velocity field  $u_i$  into the mean  $\bar{u}_i$  and fluctuation  $u'_i$  is referred to as Reynolds decomposition and can be written as (Pope 2000)

$$u_i = \bar{u}_i + u'_i. \quad (2.6)$$

Taking the Reynolds decomposition in equation (2.6), substituting it for  $u_i$  and  $u_j$ , and taking the average, the nonlinear advective term on the left-hand side of the governing Navier-Stokes equations in equation (2.1) can be expressed as

$$\overline{\frac{\partial}{\partial x_j} [(\bar{u}_i + u'_i)(\bar{u}_j + u'_j)]} = \frac{\partial}{\partial x_j} (\bar{u}_i \bar{u}_j) + \frac{\partial}{\partial x_j} (\overline{u'_i u'_j}), \quad (2.7)$$

where the velocity covariances  $\overline{u'_i u'_j}$  that arise due to the Reynolds decomposition on the right-hand side of equation (2.7) are called the Reynolds stresses.

Applying Reynolds decomposition to the other variables in equation (2.1) (i.e.  $u_i$ ,  $p$ , and  $\rho$ ), taking the average of each of the other terms, and writing the Reynolds stress tensor on the right-hand side the mean momentum equations, or Reynolds-averaged Navier-Stokes equations, become

$$\frac{\partial \bar{u}_i}{\partial t} + \frac{\partial}{\partial x_j} (\bar{u}_i \bar{u}_j) = -\frac{1}{\rho_0} \frac{\partial \bar{p}}{\partial x_i} + \nu \frac{\partial^2 \bar{u}_i}{\partial x_j \partial x_j} - \frac{\bar{\rho}}{\rho_0} g \delta_{i3} - \frac{\partial}{\partial x_j} (\overline{u'_i u'_j}). \quad (2.8)$$

Equation (2.8) is similar to the Navier-Stokes equations for conservation of momentum in equation (2.1) except for the addition of the last term on the right-hand side of Equation (2.8) from the Reynolds decomposition – the Reynolds stress tensor. This term is key and accounts for the different behavior observed between the average turbulent velocity field  $\bar{u}_i$  and the instantaneous turbulent velocity field  $u_i$ . The Reynolds stress tensor arises from the mean momentum flux due to fluctuating velocity on the boundary of a defined control volume (Pope 2000). Reynolds decomposition and averaging can also be applied to the incompressible form of the continuity equation in equation (2.4), yielding the mean continuity equation that can be expressed as

$$\frac{\partial \bar{u}_i}{\partial x_i} = 0. \quad (2.9)$$

While the Reynolds decomposition allows for the mean turbulent velocity field to be defined by a tractable set of equations amenable to numerical discretizations, it also introduces a fifth unknown term to be solved for, the Reynolds stresses  $\overline{u'_i u'_j}$ . In addition to the three mean velocity components  $\overline{u}_i$  and the mean pressure  $\overline{p}$ , the Reynolds stress tensor  $\overline{u'_i u'_j}$  is also unknown. Given the three RANS equations (e.g.  $x$ -,  $y$ -, and  $z$ -RANS equations in Cartesian coordinates) for conservation of momentum in equation (2.8) and the mean continuity equation for conservation of mass in equation (2.9), there are ten unknown variables in the four governing equations. This set of four equations with ten unknown variables results in an unclosed set of equations and is known the closure problem in turbulence when it comes to mathematical and computer modeling of the governing momentum and continuity equations. In order to solve these equations, the Reynolds stresses must be resolved (Pope 2000).

In a similar manner, a conserved passive scalar  $\phi$ , as governed by equation (2.5), can also be described as in terms of its mean  $\overline{\phi}$  by Reynolds decomposition and averaging. Hence, the Reynolds-averaged mean scalar conservation equation can be written as

$$\frac{\partial \overline{\phi}}{\partial t} + \frac{\partial}{\partial x_i} (\overline{\phi \overline{u}_i}) = \Gamma \frac{\partial^2 \overline{\phi}}{\partial x_i \partial x_i} - \frac{\partial}{\partial x_i} (\overline{\phi' u'_i}), \quad (2.10)$$

where the last term in equation (2.10) is called the scalar flux  $\overline{\phi' u'_i}$  and is analogous to the Reynolds stresses  $\overline{u'_i u'_j}$  in the Reynolds equations in the fact that it is an additional

unknown term that causes a closure problem for solving equation (2.10). Even if the mean velocity field  $\bar{u}_i$  is known, equation (2.10) cannot be solved for  $\bar{\phi}$  without determining  $\overline{\phi'u'_i}$  (Pope 2000).

Again, Reynolds decomposition and time-averaging provide a tractable and more economic approach to solving the partial differential equations that govern the motion of fluid flow. The information pertinent to most engineering problems and designs, namely the mean quantities of the flow, can be solved for in a much more concise and less costly manner than the rigorous solution of the complete set of governing equations. However, the caveat for this solution method is the emergence of the extra unknown Reynolds stress and scalar flux terms introduced by the Reynolds averaging process that must be solved for. Methods for modeling and determining the unknown terms in the Reynolds equations and closing the system of time-averaged governing equations are further discussed in the following sections and are an active subject of research in the turbulence modeling community.

## **2.4 Numerical Modeling Techniques**

There are many techniques and methods to model and predict turbulent flows that in one way or another numerically solve the partial differential equations that govern a particular turbulent flow. Some of these methodologies directly simulate the flow equations and attempt to account for many or all of the physical processes and details of the flow while others use models and assumptions (e.g. linearizing the governing equations, assuming homogeneity in one or two directions such that the flow being

analyzed becomes one- or two-dimensional, etc.) to simplify the mathematical rigor and complexity of the problem and obtain approximate solutions of the Navier-Stokes equations.

The highest and most accurate level of turbulence simulation is direct numerical simulation (DNS). In DNS, the instantaneous velocity field is obtained by solving the Navier-Stokes equations without the use of averaging or approximation for one realization of the flow. All of the fluctuations and details of the flow, including the lengthscales and timescales, are resolved to their smallest level. As one can imagine, this method is computationally expensive and is limited to idealized problems where the geometry is simple and the Reynolds number  $Re$  is low (i.e. the flow is not highly turbulent). The Reynolds number is perhaps the most limiting factor in DNS as computational cost directly increases as  $Re^3$  (Pope 2000). DNS is too expensive to be employed as a design or analysis tool for most engineering problems and the detail contained in the results of a DNS is far greater than any engineer needs. However, DNS can be useful as a research tool in the fact that it provides understanding to the physics of turbulence and the DNS data may be regarded as the equivalent of experimental data (Ferziger & Peric 2002). As computer technology has advanced, so has the ability to simulate flows of increasing complexity and higher Reynolds numbers. For example, compressible flows and stratified turbulent channel flows, such as the DNS performed by García-Villalba and del Álamo (2009), are becoming increasingly feasible with today's computing technology. Although generating DNS data is very time-consuming and computationally expensive, it has provided remarkable contributions and insight to the area of turbulence research. The ability to control and simulate a desired flow provides

valuable data that can be used to readily test new ideas and theories (Moin & Mahesh 1998).

Another simulation approach that is below the level of strictness of DNS is the large-eddy simulation (LES) technique. LES is a hybrid approach in which the equations are directly solved for a filtered velocity field, of which only the larger scales of turbulent motion that are more energetic and are directly affected by the boundary conditions are meticulously computed and solved for. The smaller scales of motion are assumed to be nearly universal in their statistics and effects on the larger scale motions of the flow and are thus modeled and specified by a small number of parameters. The theory of LES then is this, that turbulence calculations can more easily be closed by truncating scales of motion smaller than a specified grid size of interest rather than statistical moments (Rogallo & Moin 1984). DNS is the preferred simulation method because of its accuracy and simplicity, but for flows in which the Reynolds number is too high or the geometry is too complex for a DNS, LES is an advantageous method. LES has proved to be very useful in modeling certain types of flows, such as highly turbulent wall bounded flows, in which DNS is computationally impossible and simpler models are not sufficient enough to provide accurate results (Ferziger & Peric 2002).

On the opposite end of the spectrum of DNS are the various Reynolds-averaged Navier-Stokes (RANS) turbulence models that solve the Reynolds equations to determine the mean velocity field. Again in RANS models, the mean terms of the governing equations are expressed via Reynolds averaging of the instantaneous terms, by which the unsteadiness is averaged out and regarded as part of the turbulence. Due to the nonlinearity of the Navier-Stokes equations, the averaging process gives rise to the

closure problem in which the extra Reynolds stress terms and/or the scalar flux term must be modeled. Since the RANS equations give time-averaged solutions to modeled equations that attempt to account for all the complexities of turbulence, it is important to remember that RANS models are engineering approximations rather than scientific laws. Nevertheless, RANS models can effectively be used to practically model and design numerous types of environmental and engineering turbulent flows, providing quantitative properties about the flow such as velocity distribution, hydrodynamic forces, and the mixing of two or more substances (Ferziger & Peric 2002).

One approach taken to solve the Reynolds-averaged equations is to solve model transport equations for the individual Reynolds stresses. This type of model is called simply a Reynolds-stress model and requires the solution of six extra equations to close the loop and solve for the unknown Reynolds stress tensor. Still there are other RANS turbulence models consisting of zero, one, or two additional partial differential or algebraic equations that attempt to describe the effect of the Reynolds stresses on the flow. One way of determining the unknown Reynolds stresses in the mean momentum equation given in equation (2.8) is to use a turbulence model defined by the turbulent-viscosity hypothesis, which states that the unknown deviatoric Reynolds stress tensor  $\overline{u'_i u'_j}$  is proportional to the mean rate of strain as

$$\overline{u'_i u'_j} = \frac{2}{3} k \delta_{ij} - \nu_t \left( \frac{\partial \bar{u}_i}{\partial x_j} + \frac{\partial \bar{u}_j}{\partial x_i} \right). \quad (2.11)$$

If the turbulent-viscosity hypothesis is an acceptable approximation of the unknown terms for a given flow, then the Reynolds equations can be conveniently closed because the Reynolds stresses then take on a similar form to the diffusion term in the Navier-Stokes equations. All that is left then is to specify the turbulent or eddy viscosity  $\nu_t$ , which can be written as a product of a velocity scale and a lengthscale or otherwise defined to satisfy dimensional consistency (Pope 2000).

Depending on the type of flow, desired accuracy, and economy of the turbulence model, the velocity scale and lengthscale can be specified as simple algebraic models, such as the mixing-length model, or as more complex two-equation models, such as the  $k$ - $\varepsilon$  model in which the velocity scale and lengthscale are related to the turbulent kinetic energy  $k$  and the turbulent kinetic energy dissipation rate  $\varepsilon$ , for which modeled transport differential equations are solved within the framework of the Reynolds equations (the  $k$ - $\varepsilon$  model will be discussed in greater detail in chapter four). The  $k$ - $\varepsilon$  model (two equations),  $k$ - $\omega$  model (two equations), and Spalart-Allmaras model (one equation) are each examples of RANS models that are used to solve turbulent flows for different applications. The turbulent-viscosity hypothesis has been shown to be a reasonable model in solving many types of simple turbulent shear flows (e.g. channel flow and boundary layers). However, there are many types of flows (e.g. contracting flows) for which the accuracy of the turbulent-viscosity hypothesis and other simplified models is not good enough. Whatever the approach taken for a given turbulent flow problem, the method must be evaluated and appraised given the goals, limitations, and application of the problem and the model (Pope 2000).

Using the same approach as the turbulent-viscosity hypothesis for the Reynolds stresses  $\overline{u'_i u'_j}$ , the gradient-diffusion hypothesis provides a model for the scalar flux term in equation (2.10). The gradient-diffusion hypothesis states that the scalar flux  $\overline{\phi' u'_i}$  is aligned with and proportional to the mean scalar  $\bar{\phi}$  gradient as

$$\overline{\phi' u'_i} = -\Gamma_t \frac{\partial \bar{\phi}}{\partial x_i}. \quad (2.12)$$

Again the Reynolds-averaged mean scalar conservation equation can be closed, provided a model for the turbulent or eddy scalar diffusivity  $\Gamma_t$  is specified. Like the eddy viscosity  $\nu_t$ , the scalar eddy diffusivity  $\Gamma_t$  is commonly defined as the product of the square of a velocity scale and a lengthscale such that dimensional consistency is satisfied. Just as with the turbulent-viscosity hypothesis, the gradient-diffusion hypothesis is not without its limitations. Both hypotheses imply physical meanings that do not always hold true, but for certain flows can yield accurate and attainable solutions to the modeled equations (Pope 2000).

## 2.5 Relevant Parameters of Stratified Turbulent Flows

While there are many parameters that specify and define turbulent stratified fluid flows (many of which will be discussed in this section), a single non-dimensional parameter called the Reynolds number  $Re$  is fundamental to characterizing fluid flow. The Reynolds number is a dimensionless number that defines the ratio of inertial forces

to viscous forces in a fluid flow and can be expressed as the product of a velocity scale  $U$  and a lengthscale  $L$  divided by the kinematic viscosity of the fluid  $\nu$  as

$$Re = \frac{UL}{\nu}. \quad (2.13)$$

In all types of flows, the Reynolds number can be used to describe a threshold for turbulence and the phenomena associated with it. For example, the range of scales and fine structures seen within a flow is related to the Reynolds number. At high Reynolds numbers ( $>10000$ ), a large range of scales is observed (Pope 2000).

The Froude number  $Fr$  is another dimensionless parameter that is defined as the ratio of inertial forces to gravitational forces in a fluid and is given by

$$Fr = \frac{U}{\sqrt{gL}}. \quad (2.14)$$

The Froude number is an important parameter for flows with a free surface and in which gravity forces are dynamically significant. In a density stratified fluid the gravity force can still influence the flow even if there is no free surface. The effective gravity force in a stratified fluid is a buoyant force caused by the density gradient. An internal Froude number  $Fr'$  describing the ratio of inertial forces to buoyant forces can then be defined as (Kundu 1991)

$$Fr' = \frac{U}{NL}, \quad (2.15)$$

where  $N$  is the Brunt-Väisälä or buoyancy frequency and describes the frequency at which a parcel of fluid vertically displaced from its equilibrium position in a stable environment will oscillate due to buoyant and gravitational forces. The buoyancy frequency can be defined as a function of the mean density gradient in a stratified flow as

$$N = \left( -\frac{g}{\rho_0} \frac{\partial \bar{\rho}}{\partial z} \right)^{1/2}. \quad (2.16)$$

A dimensionless parameter called the gradient Richardson number  $Ri$  is often used instead of  $Fr'$  to characterize the strength of stratification of the flow, computed from values of the mean shear rate or velocity gradient  $S = d\bar{u}/dz$  and buoyancy frequency  $N$  at a certain depth within the flow as

$$Ri = \frac{N^2}{S^2}. \quad (2.17)$$

The gradient Richardson number is an important parameter in describing stability and understanding turbulent mixing in stratified flows (Kundu 1990).

The Prandtl number  $Pr$  is a fundamental dimensionless parameter of fluid flows, approximating the ratio of molecular momentum diffusivity  $\nu$  to heat or scalar diffusivity  $\Gamma$ . The Schmidt number  $Sc$  is analogous to the Prandtl number and sometimes used

instead to specifically describe mass transfer instead of heat transfer. Here, the Prandtl number  $Pr$  is defined as

$$Pr = \frac{\nu}{\Gamma}. \quad (2.18)$$

It is important to note that the Prandtl number is strictly a function of fluid properties and not dependent upon the specification of a flow variable such as a lengthscale or velocity scale as with each of the other parameters discussed above (White 1991).

In the case of momentum transfer and mixing in turbulent fluid flows, a turbulent Prandtl number  $Pr_t$  may be analogously defined as the ratio of the eddy viscosity  $\nu_t$  to the scalar eddy diffusivity  $\Gamma_t$  that are introduced by the turbulent-viscosity hypothesis in equation (2.11) and the gradient-diffusion hypothesis in equation (2.12) respectively. Here,  $Pr_t$  is a flow-dependent parameter and is written as

$$Pr_t = \frac{\nu_t}{\Gamma_t}. \quad (2.19)$$

For neutrally stratified flows,  $Pr_t$  has been found to be a constant of order unity. In the case of stratified flows,  $Pr_t$  cannot be considered to be a constant value but rather it depends on buoyancy effects and is often expressed in terms of one or more other parameters that define the degree of stratification of the flow. These are just some of the most prevalent parameters used in describing and modeling turbulent and/or stratified fluid flows. Other important modeling parameters used in this research depend on the

specific model and approach chosen to investigate a certain flow and will be defined as they are introduced in subsequent sections of this thesis.

## **2.6 Characteristics of Stratified Flows**

The attributes of the density gradient that characterizes a stratified flow will affect the behavior and mixing properties of the flow. The buoyancy frequency  $N$  and the gradient Richardson number  $Ri$  that are defined in the previous section are parameters that describe the strength of the stratification of the flow. There are other factors such as stability, layering, and active scalar coupling that also determine how a stratified flow will evolve and how it should be modeled to reflect the physics of stratified turbulence. The challenge of describing parameters and adjusting models to account for the buoyant forces that affect stratified flows starts with an understanding of the interaction between the two.

Density stratification can either be described as stable or unstable depending on the direction of increasing mean fluid density with respect to depth of the flow. When the mean fluid density increases with depth and the heavier fluid is below the lighter fluid, the density stratification is stable. Therefore, any disturbance will simply result in a restoring force. When the mean fluid density decreases with depth, the stratification is unstable and any displacement will cause an instability resulting in an overturning (destabilizing) force. Both scenarios are visualized in figure 2.1 (Turner 1973).

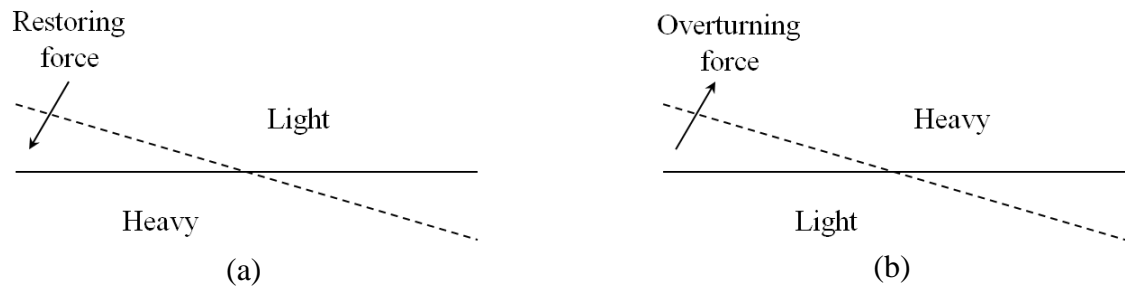


**Figure 2.1.** Displacements from hydrostatic equilibrium: (a) stable; and (b) unstable density distributions.

In addition to variations in stability, density stratification can be characterized by a gradient that is continuous or layered, affecting fluid motion and mixing. In a continuously stratified fluid, such as the deep ocean, the density gradient is relatively constant over the entire depth of the flow as shown by the profile in figure 2.2(a). Layered stratification, occurring in lakes, reservoirs, and atmospheric inversion layers, consists of two or more well-mixed layers of relatively constant density separated by a distinct interface and is depicted in figure 2.2(b). The interface of these layers forms a sharp density gradient within the flow, often referred to as a pycnocline or thermocline.

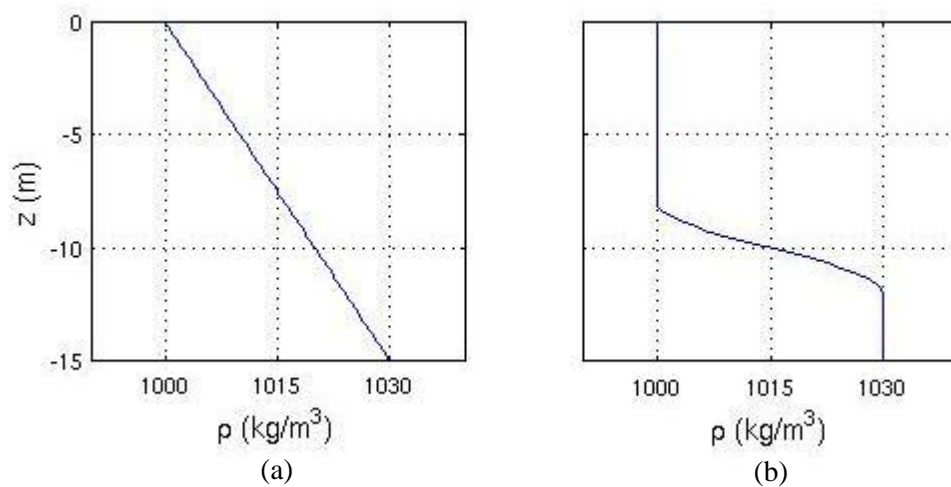


**Figure 2.2.** Density profiles: (a) continuous stratification density profile; and (b) two-layered stratification density profile.

The buoyancy forces present in stratified flows can either act as an energy sink or as an energy source in the turbulence depending on the stability condition. The overturning force present in unstable stratification works with turbulence to transport and mix the fluid whereas the restoring force present in stably stratified flows acts to extract energy, working against the production of turbulent kinetic energy to reduce turbulent transport and mixing. The latter is especially true in the case of a stably stratified flow where the production of turbulent energy is generated mainly due to shear stress at the bottom boundary (e.g. channel flow). The turbulence generated by shear at the boundary that lends itself to momentum transfer and mixing becomes more suppressed in the interior part of the flow where buoyancy effects due to stratification become dominant. The parameter defining the transfer of energy in stratified turbulent flows is the buoyancy flux  $B$  and is defined as

$$B = -\frac{g}{\bar{\rho}} \overline{\rho'w'}, \quad (2.20)$$

where  $\rho'$  and  $w'$  are the fluctuations of density and vertical velocity respectively (Turner 1973). The sign of  $B$  is dictated by whether the stratification is stable or unstable and accounts for the addition or subtraction of turbulent kinetic energy to or from the flow. The buoyancy flux term's role in the complete turbulent kinetic energy budget equation is discussed further in regards to the  $k$ - $\varepsilon$  model in chapter four.

The buoyant forces due to density stratification also present a challenge to modeling stratified flows because the density  $\rho$  is an active scalar that in part influences and drives the flow as opposed to being passively transported by the flow. As a

dynamically active scalar, the Reynolds-averaged scalar equation for  $\rho$  is coupled to the Reynolds-averaged momentum equation via the scalar flux term in equation (2.10) and the Reynolds stresses and fluctuating body force term in equation (2.8) respectively. The fluctuating body force in the vertical momentum equation is caused by buoyant forces and affects both the mean flow field and the turbulence. Thus, the momentum equation cannot be solved independently of the scalar conservation equation for density.

## 2.7 Conclusions

This chapter has introduced the fundamental equations and parameters governing and describing stratified turbulent flows. Models attempt to obtain solutions to stratified turbulent flows by modifying key parameters and variables in the equations, some of which have been discussed in this chapter, to imitate the effects of stratification on turbulence. Some models vary parameters and variables as functions of stratification parameters such as the gradient Richardson number  $Ri$  while others may rely on simple empirical constants to reflect laboratory or field data (Durbin & Pettersson Reif 2001). The work of this thesis explores each of these methods while also attempting to test new descriptions of parameters to characterize stratification in turbulence models. Further reviews of stably stratified environmental flows are given by Gregg (1987), Fernando (1991), Riley and Lelong (2000), Peltier and Caulfield (2003), and Ivey *et al.* (2008). In what follows in the next chapter of this thesis, the effects of stratification on turbulent flow development and scalar transport are explored using a zero-equation turbulence model in one-dimensional turbulent channel flow.

# CHAPTER 3

## EVALUATION OF TURBULENT PRANDTL NUMBER PARAMETERIZATIONS USING A ZERO-EQUATION TURBULENCE MODEL<sup>1</sup>

### 3.1 Introduction

The complexity of a turbulence model used to capture and represent as many or all of the physics of a turbulent flow can range from simple to elaborate depending on the nature of the flow and its application. Sometimes, a basic example coupled with a simple model used to understand the fundamentals of fluid dynamics and turbulence can shed insight and understanding into deeper and more complicated problems. Thus, using a somewhat arbitrary but strong test case, the simple case of a one-dimensional stratified channel flow in which the density profile is held fixed in the channel is used to study the effects of stable stratification on turbulent flow development and mixing. In this chapter, the focus is primarily on the relationship between the turbulent Prandtl number  $Pr_t$  and the strength of stratification of the flow as characterized by the gradient Richardson number  $Ri$ . A zero-equation turbulence model for shallow flows in an equilibrium state of

---

<sup>1</sup> This chapter is in press for publication in substantial part as “Evaluation of turbulent Prandtl (Schmidt) number parameterizations for stably stratified environmental flows” by Z.A. Elliott and S.K. Venayagamoorthy in *Dynamics of Atmospheres and Oceans* (2010), doi:10.1016/j.dynatmoce.2011.02.003.

turbulence is used to quantify the behavior of four different formulations of  $Pr_t$  under multiple stratification and flow conditions. Both uni-directional and oscillatory flows are considered to simulate conditions representative of practical flow problems such as atmospheric boundary layer flows and tidally-driven estuarine flows. The results are used to evaluate which of the models of  $Pr_t$  allow for a higher rate of turbulent mixing and which models significantly inhibit turbulent mixing in the presence of buoyancy forces resulting from fixed continuous stratification as well as fixed two-layer stratification. The basis underlying the formulation of each model in conjunction with the simulation results are used to emphasize the considerable variability in the different formulations and the importance of choosing an appropriate parameterization of  $Pr_t$ , given a model for the eddy viscosity  $\nu_t$  in stably stratified flows.

### 3.2 Problem Set-Up

Assuming a one-dimensional, fully developed turbulent channel flow with a hydrostatic pressure distribution and a logarithmic velocity profile, a parabolic eddy viscosity model for  $\nu_t$  as a function of the flow depth  $z$  can be derived for a neutrally stable case by using a momentum balance between the horizontal pressure gradient and turbulent shear stress (vertical mixing) in conjunction with the Boussinesq turbulent-viscosity hypothesis as (Rodi 1993)

$$\nu_t(z) = \kappa u_\tau (-z/H)(H+z), \quad (3.1)$$

where  $\kappa$  is the von Karman constant (taken as  $\kappa = 0.41$ ),  $u_\tau$  is the shear or friction velocity,  $H$  is the total flow depth in the channel, and  $z = 0$  at the free surface. The simple parabolic eddy viscosity model given by equation (3.1) only accounts for turbulence generated at the bottom boundary of the channel by the bed friction, but can still be effectively used for fully developed channel flows.

Because stable stratification in the channel can significantly limit the vertical turbulent mixing away from the channel bed, the parabolic eddy viscosity model given in equation (3.1) can be modified in the presence of stable stratification according to a model proposed by Munk and Anderson (1948). Their algebraic model for the modified eddy viscosity  $\nu_{t|\text{mod}}$  accounts for the vertical effect of the buoyancy forces caused by stable stratification by describing  $\nu_{t|\text{mod}}$  as a function of  $Ri$  and the flow depth  $z$  as

$$\nu_{t|\text{mod}}(z) = \nu_t (1 + \beta Ri)^\alpha, \quad (3.2)$$

where  $\beta$  and  $\alpha$  are experimentally determined constants with given values of 10 and -1/2 respectively (Munk & Anderson 1948). It is clear that the value of  $\nu_{t|\text{mod}}$  is significantly reduced where there is a strong density gradient in the flow limiting the turbulent mixing. However, Munk and Anderson's model given by equation (3.2) does not account for the suppression of turbulence generated at the channel bed in fluid layers above a pycnocline in the case of two-layer stratification where the density may again become relatively constant up to the free surface. Thus, it is not reasonable to let the eddy viscosity be unaffected above the pycnocline since the only source of turbulence is assumed to be from the bottom shear stress. Therefore in the presence of a pycnocline, it is reasonable to

further adapt the model for  $\nu_t|_{\text{mod}}$  by limiting the eddy viscosity above the pycnocline to a cut-off value less than the value of  $\nu_t|_{\text{mod}}$  computed at the mid-depth of the pycnocline from equation (3.2). Above the pycnocline then,  $\nu_t|_{\text{mod}}$  is modeled as a parabolic function, decreasing from the value of  $\nu_t|_{\text{mod}}$  computed at the mid-depth of the pycnocline to zero at the free surface (personal communication, Robert L. Street). This is given by

$$\nu_t|_{\text{mod}}(z) = \nu_t|_{\text{mod},\text{pyc}} \left( \frac{z}{z_{\text{pyc}}} \right) \left( 2 - \frac{z}{z_{\text{pyc}}} \right) \quad \text{for } z > z_{\text{pyc}}, \quad (3.3)$$

where  $z_{\text{pyc}}$  is the mid-depth of the pycnocline and  $\nu_t|_{\text{mod},\text{pyc}}$  is the value of  $\nu_t|_{\text{mod}}$  computed at the mid-depth of the pycnocline from equation (3.2). This approach, designated as the modified Munk and Anderson (1948) cut-off model, is admittedly simple but it mimics the suppression of turbulent mixing generated at the channel bed above the sharp density gradient while still modeling  $\nu_t|_{\text{mod}}$  as a parabolic shape as derived in equation (3.1).

Accepting the modified Munk and Anderson (1948) formulation as a model for the eddy viscosity  $\nu_t$ , different formulations of  $Pr_t$  and its effect on the scalar eddy diffusivity  $\Gamma_t$  and mixing of a passive scalar in stably stratified flows were then investigated by simulating a simple one-dimensional channel flow. The flow was assumed to be fully developed and one-dimensional such that the flow variables are horizontally homogeneous and characterized by either a constant, continuous vertical density gradient or a sharp density gradient interface separating two fluid layers of relatively constant density akin to flow in a coastal estuary channel or an atmospheric boundary layer as shown in the schematic of the problem set-up in figure 3.1. A somewhat artificial test case was used in that the density profile was held fixed in time, in

some ways similar to the simulations and experiments done by Venayagamoorthy *et al.* (2003) and Komori *et al.* (1983). Hence, the calculations assume that the density profile is unchanged by the turbulent mixing that occurs, illustrating a situation where the stratification is very strong and/or that the mixing takes place in much shorter timescales than the effect of turbulence on the stratification. For this simple one-dimensional flow, the horizontal terms can be ignored since the balance is primarily between the pressure gradient and vertical turbulent mixing. Hence, the governing equations are a form of the horizontal momentum equation coupled with a prescribed forcing equation that can be used as a periodic function to model the effect of the ebb and flow of a tide in an estuary. These equations are given respectively as

$$\frac{\partial u}{\partial t} = -g \frac{\partial \eta}{\partial x} + \frac{\partial}{\partial z} \left[ \nu_t \frac{\partial u}{\partial z} \right] \quad (3.4)$$

and

$$\frac{\partial \eta}{\partial x} = -\frac{U_{\max}}{g} \left( \frac{2\pi}{T} \right) \cos \left( \frac{2\pi}{T} t \right), \quad (3.5)$$

where  $\eta$  is the free surface elevation,  $T$  is the period of the semi-diurnal tide (i.e. 12.42 hours for a  $M_2$  tidal constituent), and  $U_{\max}$  is a prescribed maximum velocity of the flow in the channel. The scalar diffusion equation used to model the change in concentration of a passive scalar  $C$  over the depth of the channel in time is given by

$$\frac{\partial C}{\partial t} = \frac{\partial}{\partial z} \left[ \Gamma_t \frac{\partial C}{\partial z} \right], \quad (3.6)$$

where  $\Gamma_t$  is the scalar eddy diffusivity computed from the modified Munk and Anderson (1948) formulation of  $\nu_t$  and a given formulation of  $Pr_t$  as a function of  $Ri$ .

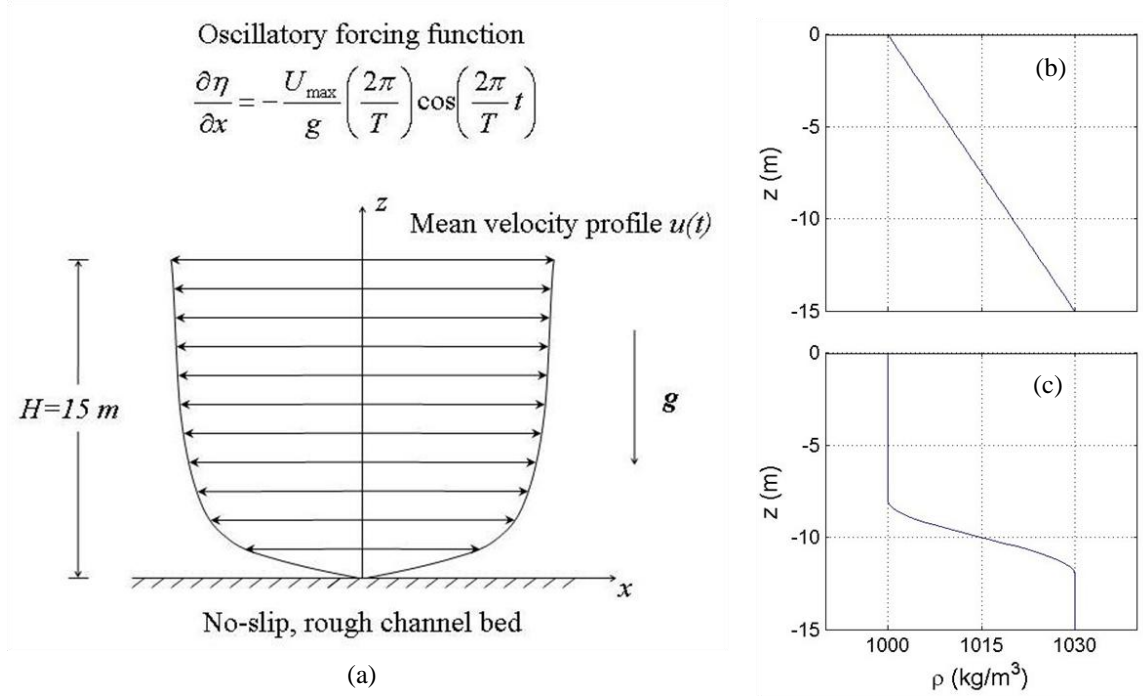


**Figure 3.1.** Schematic of the problem set-up depicting (a) the tidal velocity field; (b) a continuous stratification density profile; and (c) a two-layered stratification density profile.

The governing partial differential equations (PDEs) given in equations (3.4) – (3.6) are more amenable to numerical solutions than analytical solutions since the eddy viscosity depends on  $Ri$ , which can vary with depth over a wide range of values. Equations (3.4) – (3.6) must therefore be discretized in space and time to obtain solutions. The accuracy of the discretization scheme chosen is based on the order of the terms that are retained from a Taylor series expansion of the derivative terms. For this

model, a second-order accurate, central-differencing scheme based on a finite volume formulation was used to approximate the spatial derivatives. Substituting equation (3.5) into equation (3.4) and discretizing the remaining spatial term according to the method described above yields

$$\frac{\partial u}{\partial t} = U_{\max} \left( \frac{2\pi}{T} \right) \cos \left( \frac{2\pi}{T} t \right) + \frac{[v_{t_{i+1/2}}(u_{i+1} - u_i) - v_{t_{i-1/2}}(u_i - u_{i-1})]}{\Delta z^2}, \quad (3.7)$$

where the subscripts on the discretized terms are indices denoting spatial grid points. The spatial discretization of the scalar diffusion equation given in equation (3.6) using a similar scheme yields

$$\frac{\partial C}{\partial t} = \frac{\Gamma_{t_{i+1/2}}(C_{i+1} - C_i) - \Gamma_{t_{i-1/2}}(C_i - C_{i-1})}{\Delta z^2}. \quad (3.8)$$

A semi-implicit discretization scheme known as the  $\theta$ -method was used to approximate the temporal derivatives of the horizontal momentum equation as

$$\left. \frac{\partial u}{\partial t} \right|_i^{n+\theta} = U_{\max} \left( \frac{2\pi}{T} \right) \cos \left( \frac{2\pi}{T} t \right)_i^{n+\theta} + \frac{\partial}{\partial z} \left[ v_t \frac{\partial u}{\partial z} \right]_i^{n+\theta}, \quad (3.9)$$

where the superscripts on the discretized terms are indices denoting temporal grid points or time steps. The scalar diffusion equation can be discretized in time via the  $\theta$ -method as

$$\left. \frac{\partial \mathcal{C}}{\partial t} \right|_i^{n+\theta} = \frac{\partial}{\partial z} \left[ \Gamma_t \left. \frac{\partial \mathcal{C}}{\partial z} \right]_i^{n+\theta} . \quad (3.10)$$

The  $\theta$ -method makes use of the implicitness parameter  $\theta$  to improve the accuracy and efficiency of the scheme (Casulli & Cattani 1994). The objective of the  $\theta$ -method is to give more or less weighting to the implicit terms in the discretized equation, or the unknown terms being evaluated for the next time step  $n+1$  in the time-marching solution algorithm as

$$t^{n+\theta} = [\theta t^{n+1} + (1-\theta)t^n]. \quad (3.11)$$

This weighting of implicit terms is based on the value of  $\theta$ , which can range anywhere from 0 to 1. If  $\theta = 0$ , then the scheme is fully explicit and first-order accurate in time and there are no implicit terms to be solved for in the equation. Conversely, if  $\theta = 1$ , then the scheme is fully implicit and first-order accurate in time and there is no weight given to the explicit terms. However, if  $\theta$  takes a value between 0 and 1, the scheme becomes semi-implicit and between first- and second-order accurate in time. When  $\theta = 0.5$ , variables in the governing equations are evaluated as an average of their values at time levels  $n$  and  $n+1$  so that the discretization is second-order accurate in time (known as the Crank-Nicolson scheme). The method has been shown to be stable for  $0.5 \leq \theta \leq 1$ , with second-order time accuracy for  $\theta = 0.5$ . When  $\theta < 0.5$ , the method is only conditionally stable (Casulli & Cattani 1994). It has been shown that a value of  $\theta$  slightly greater than

0.5 can be used in order to dampen and eliminate high-frequency oscillations (i.e. obtain asymptotic stability) without adversely affecting the simulations with numerically induced diffusion (Fringer *et al.* 2006). It was found for this problem that a value of  $\theta \approx 0.7$  produced oscillation-free solutions.

Combining the spatial and temporal discretizations of the horizontal momentum equation given in equations (3.7) and (3.9) and the scalar diffusion equation given in equations (3.8) and (3.10) yields the set of difference equations used to approximate the governing equations given in equations (3.4) – (3.6). These difference equations are finite algebraic equations that represent continuous PDEs and can be solved on a computer at a set of discrete locations or points in space and time.

In order to completely define and be able to solve the set of discretized equations, initial and boundary conditions must be defined to start the solution algorithm and relate it to the system in which it is being analyzed. To initialize the velocity field of the flow at some starting point in time for the uni-directional channel flow, the model was spun up and the flow was allowed to reach a fully developed turbulent velocity profile before the passive scalar  $C$  was released in the flow. For the case of the tidally driven channel flow, the velocity in the channel was set to zero and allowed to be initialized by the effect of the periodic tidal forcing function defined in (3.5). Consequently, the variation with depth of  $v_t|_{\text{mod}}$  in the channel, being a function of the shear velocity near the channel bed, is dictated by the prescribed initial velocity field of the flow. Flux (or Neumann) boundary conditions at the free surface and at the bed were specified to completely define the problem. At the free surface, wind shear was not considered and hence the velocity gradient in the vertical direction was assumed to be zero due to the expected behavior of

the log-law velocity profile to reach a maximum value near the free surface. At the channel bed, the effects of a rough bed and a viscous boundary layer are given by the drag law to represent the shear stress at the boundary (Fringer *et al.* 2006). The velocity gradient in the vertical direction was modeled as a function of the drag coefficient  $C_D$  (which depends on the channel roughness),  $\nu_t$  at the boundary, and the flow velocity near the boundary  $u_1$  given as

$$\left. \frac{\partial u}{\partial z} \right|_{z=-H} = \frac{C_D}{\nu_t} |u_1| u_1, \quad (3.12)$$

where  $u_1$  is the mean flow velocity at the first grid point from the lower boundary or bed of the channel. It is important to note that for real flows with rough boundaries a wall point to define the no-slip condition where the velocity goes to zero cannot be consistently defined due to the irregular roughness elements of the channel bed. Therefore, the boundary condition was applied some distance away from the actual boundary to account for the roughness elements of a real channel. The maximum velocity in the channel  $U_{\max}$  was prescribed for each case such that the maximum value of  $\nu_t|_{\text{mod}}$  reached in the channel was the same for both the uni-directional channel flow case and the oscillatory channel flow case. This corresponds approximately to a friction Reynolds number of  $Re_\tau = u_\tau H / \nu = 273300$  and a friction Richardson number  $Ri_\tau = (NH/u_\tau)^2 = 13300$  for the continuously stratified uni-directional flow simulations and  $Re_\tau = 386000$  and  $Ri_\tau = 6670$  for the two-layered stratified uni-directional flow simulations.  $Re_\tau = 335000$  and  $Ri_\tau = 8880$  for the continuously stratified oscillatory case (based on the

maximum value of  $u_\tau$  reached at the peak of the ebb or flood cycle) and  $Re_\tau = 367000$  and  $Ri_\tau = 7360$  for the two-layered stratified oscillatory flow case.

The parameters of interest in the problem including the variation in density and initial concentration and distribution of the passive scalar  $C$  must also be specified as functions of space and time. As prescribed, the flow was modeled as a stably stratified flow as either a constant, continuous density gradient or as a distinct, sharp gradient between two layers of fluids of relatively constant density as shown in figure 3.1(b) and 3.1(c) respectively. The position of the distinct pycnocline interface between the two densities can be clearly seen in figure 3.1(c). Also, the initial distribution and position of a passive scalar  $C$  was centered at three different depths in the channel for each of the two density stratifications, above the position of the pycnocline, at the position of the pycnocline, and below the position of the pycnocline as shown in figure 3.4(a) – (c) and figure 3.5(a) – (c) respectively.

With the complete set of discretized equations, initial conditions, and boundary conditions defined, a solution algorithm was developed and programmed to march the solution forward in time. Since the algorithm uses a semi-implicit time discretization scheme, the matrix of discretized equations at each grid point varying with depth in the channel must be solved simultaneously at each time step to produce a solution. To program this, a time-marching loop was coded into the algorithm to update the coefficients ( $v_i/\text{mod}$  and  $Ri$ ) at each time step so that the implicit matrix equations for velocity and concentration at the next time step could be solved. Due to the one-dimensional nature of the problem, the linear system of equations yields a tri-diagonal matrix system which can be easily solved using a sparse Gaussian elimination procedure

such as the Thomas Algorithm. All coding and output of model results was done in MATLAB (R2009, the Mathworks, Inc., Natick, MA, USA). Refer to appendix A for the MATLAB code developed for this study.

### 3.3 Turbulent Prandtl Number Formulations

Four different formulations of  $Pr_t$  as a function of  $Ri$  were considered to study the effects of stratification on  $\Gamma_t$  as well as the vertical mixing of  $C$  in equation (3.6) given the zero-equation eddy viscosity model in equation (3.2) proposed by Munk and Anderson (1948) for the case of the linear stratification and the modified cut-off Munk and Anderson model for the two-layered stratification. A key debate in the stratified modeling community pertains to the issue of whether turbulence is completely quenched at high values of  $Ri$  (Galperin *et al.* 2007). There are a number of models for  $Pr_t$  ranging from those that propose an asymptotic maximum value for  $Pr_t$  beyond a critical value of  $Ri$  based on the concept of turbulence extinction to formulations where  $Pr_t$  continues to increase monotonically as a function of  $Ri$ . Three of the four formulations chosen for this study are based on the concept that scalar mixing is inhibited in an ever increasing manner as functions of  $Ri$  without any asymptotic leveling off of mixing. Each of the formulations of  $Pr_t$  was tested for both the continuously stratified case and the two-layered stratified case in a uni-directional flow as well as a tidally-driven oscillatory flow.

The first expression of  $Pr_t$  considered is also a formulation by Munk and Anderson (1948) (hereafter MA). They proposed a model for a modified scalar eddy

diffusivity  $\Gamma_t|_{\text{mod}}$  of the same form as  $\nu_t|_{\text{mod}}$  in equation (3.2) to account for the effect of buoyant forces given as

$$\Gamma_t|_{\text{mod}}(z) = \Gamma_t (1 + \beta_\rho Ri)^{\alpha_\rho}, \quad (3.13)$$

where  $\beta_\rho$  and  $\alpha_\rho$  are again empirical constants with prescribed values of 10/3 and -3/2 respectively (Munk & Anderson 1948).  $Pr_t$  as a function of  $Ri$  is obtained by dividing equation (3.2) by equation (3.13) to get

$$Pr_t = \frac{\nu_t}{\Gamma_t} \frac{(1 + \beta Ri)^\alpha}{(1 + \beta_\rho Ri)^{\alpha_\rho}}, \quad (3.14)$$

where  $\nu_t/\Gamma_t$  can be defined by equation (2.19) as the turbulent Prandtl number for a neutrally stratified case  $Pr_{t0}$  such that equation (3.14) can be rewritten as

$$Pr_t = Pr_{t0} \frac{(1 + \beta Ri)^\alpha}{(1 + \beta_\rho Ri)^{\alpha_\rho}}. \quad (3.15)$$

The second relationship for  $Pr_t$  based on  $Ri$  was recently derived by Venayagamoorthy and Stretch (2010) (hereafter VS) using theoretical arguments supported by DNS data for homogeneous stably stratified turbulent flows. Their model for  $Pr_t$  as a function of  $Ri$  is given as

$$Pr_t = Pr_{t0} \exp\left(-\frac{Ri}{Pr_{t0}\Gamma_\infty}\right) + \frac{Ri}{R_{f\infty}}, \quad (3.16)$$

where  $\Gamma_\infty$  is the mixing efficiency and  $R_{f\infty}$  is the asymptotic value of the flux Richardson number. The DNS results analyzed by VS indicate an average value of  $\Gamma_\infty \approx 1/3$ , which translates to  $R_{f\infty} \approx 1/4$  since these two quantities are related by  $\Gamma_\infty = R_{f\infty}/(1 - R_{f\infty})$  (Venayagamoorthy & Stretch 2010).

There has been much work and research done concerning the value of  $Pr_{t0}$  in neutrally stratified flows. Data from numerical simulations and experiments done by Kays and Crawford (1993) and Kays (1994) suggest values of  $Pr_{t0}$  between 0.5 and 1.0 for neutrally stratified flows (Kays & Crawford 1993, Kays 1994). Theoretical reasoning and DNS data analyzed by VS further suggest that  $Pr_{t0}$  is approximately equal to the ratio of the scalar timescale  $T_\rho$  to the mechanical (turbulence) timescale  $T_L$  or  $Pr_{t0} = 1/(2\gamma)$  where  $\gamma = (1/2)(T_L/T_\rho)$ . Using  $\gamma \approx 0.7$  as suggested by Venayagamoorthy and Stretch (2006) yields a value of  $Pr_{t0} \approx 0.7$ . This neutral value of the turbulent Prandtl number has been adopted for the present study.

The third formulation for  $Pr_t$  is given by Kim and Mahrt (1992) (hereafter KM). Their formulation of  $Pr_t$  is derived from the Louis model that relates the mixing length for heat to the Richardson number (Louis 1979, Louis *et al.* 1981). Using aircraft data to validate their model, KM arrive at a formulation of  $Pr_t$  similar to that of MA as

$$Pr_t = Pr_{t0} \frac{1 + 15Ri(1 + 5Ri)^{1/2}}{1 + 10Ri(1 + 5Ri)^{-1/2}}. \quad (3.17)$$

The final formulation of  $Pr_t$  is derived from expressions of  $\nu_t$  and  $\Gamma_t$  presented by Strang and Fernando (2001) from formulations by Peters *et al.* (1988) (hereafter PGT). The PGT empirical formulations of the eddy viscosity and scalar eddy diffusivity are driven by data obtained from a study of the Pacific Ocean near the equator (Peters *et al.* 1988) and given respectively as

$$\nu_t = 5.6 \times 10^{-4} \cdot Ri^{-8.2} \quad (3.18)$$

and

$$\Gamma_t = 3.0 \times 10^{-5} \cdot Ri^{-9.6} \quad (3.19)$$

for  $Ri \leq 0.25$  and as

$$\nu_t = \frac{5.0}{(1.0 + 5.0Ri)^{1.5}} + 0.2 \quad (3.20)$$

and

$$\Gamma_t = \frac{5.0}{(1.0 + 5.0Ri)^{2.5}} + 0.01 \quad (3.21)$$

for  $Ri > 0.25$  (Strang & Fernando 2001). Combining equations (3.18) and (3.19) for  $Ri \leq 0.25$  and equations (3.20) and (3.21) for  $Ri > 0.25$  respectively yields a model for  $Pr_t$  as

$$Pr_t = \frac{56}{3} Ri^{1.4} \quad \text{for } Ri \leq 0.25 \quad (3.22)$$

and

$$Pr_t = \frac{5.0(1.0 + 5.0Ri)^{-1.5} + 0.2}{5.0(1.0 + 5.0Ri)^{-2.5} + 0.01} \quad \text{for } Ri > 0.25. \quad (3.23)$$

This model of  $Pr_t$  proposed by PGT behaves differently from the other three models in that here  $Pr_t$  does not continue to grow with increasing  $Ri$ . Instead, it asymptotically approaches a maximum value of  $Pr_t \approx 20$  as  $Ri \rightarrow \infty$  (see figure 3.2). Also, it is important to note that this empirical formulation of  $Pr_t$  yields a value of 0 when  $Ri = 0$  (i.e. unstratified flow). This would imply that there is infinite turbulent mixing of a passive scalar for neutrally stratified flows. This clearly implies that this model would only be physically applicable for  $Ri > 0$  (i.e. stratified flow) as opposed to the other three formulations, which are more general in that there is a seamless transition to the unstratified case with  $Pr_t \rightarrow Pr_{t0}$  as  $Ri \rightarrow 0$ . Each of the four functions of  $Pr_t$  considered in this study are shown as a function of  $Ri$  in figure 3.2 with the upper bound value of  $Ri$  truncated at 10 for clarity.

It might appear to be obvious from figure 3.2 as to which of these models will permit greater levels of mixing or vice versa. Clearly KM has the steepest slope implying less scalar mixing while MA has the smallest slope indicating enhanced scalar mixing. However, the model by PGT suggests a much stronger suppression of scalar mixing for lower values of  $Ri$  than the rest but higher levels of mixing compared to KM for  $Ri > 4.1$ ,

VS for  $Ri > 5.2$ , and MA for  $Ri > 14.9$ . Given the large range of values of  $Ri$  that varies with flow depth in a channel flow (for a nice theoretical discussion, see Armenio and Sarkar (2002)), the mixing properties of each of the  $Pr_t$  formulations might not be immediately apparent and only through test cases like those presented here can they be best understood.

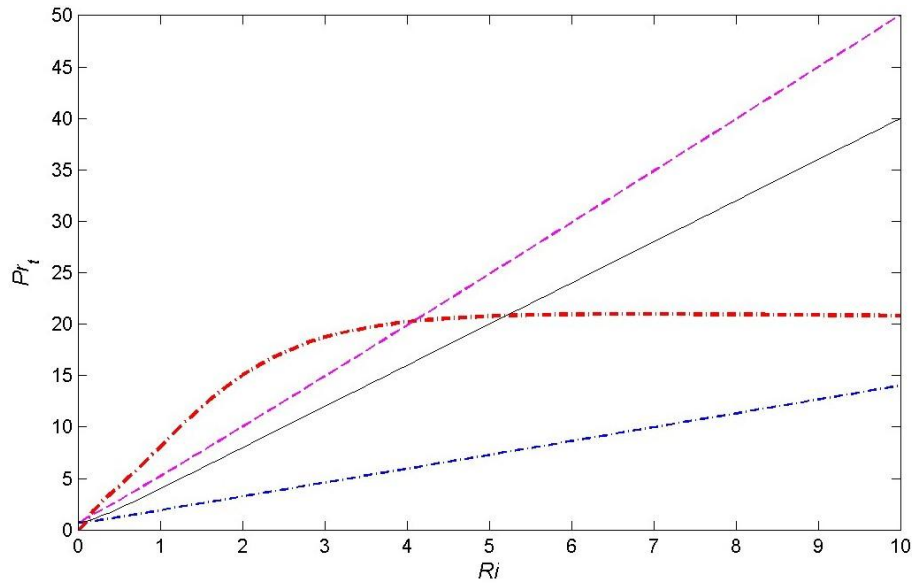


**Figure 3.2.** The turbulent Prandtl number  $Pr_t$  as a function of the gradient Richardson number  $Ri$  for four different models: blue dashed-dotted line, Munk and Anderson (1948); black solid line, Venayagamoorthy and Stretch (2010); purple dashed line, Kim and Mahrt (1992); red thick dashed-dotted line, Peters *et al.* (1988).

### 3.4 Results

All four of the  $Pr_t$  formulations were tested for the two types of stratified flow conditions shown in figures 3.1(b) and 3.1(c) for three different locations of an initial passive scalar plume  $C$  as depicted in figure 3.4(a) – (c) and figure 3.5(a) – (c) respectively. All of these cases were tested for a fully developed uni-directional stratified

channel flow and for a tidally-driven stratified channel flow in which the velocity field changes as a function of time. The results of the stably stratified flows were then compared to a base case of an unstratified flow, which is shown in figure 3.3. The unstratified cases were tested first and the model was run until the initial plume was completely mixed over the depth of the channel (see figure 3.3(c)). This took approximately 5800 seconds for both cases (approximately 0.13  $M_2$  tidal periods). The mixing of  $C$  from its initial condition for the two-layered stratified and continuously stratified cases required a period of approximately 50 ( $\approx 6.5 M_2$  tidal periods) and 100 ( $\approx 13 M_2$  tidal periods) times the time that was required for the unstratified case to mix out. A total of 18 simulations runs were performed to assess these four  $Pr_t$  models.

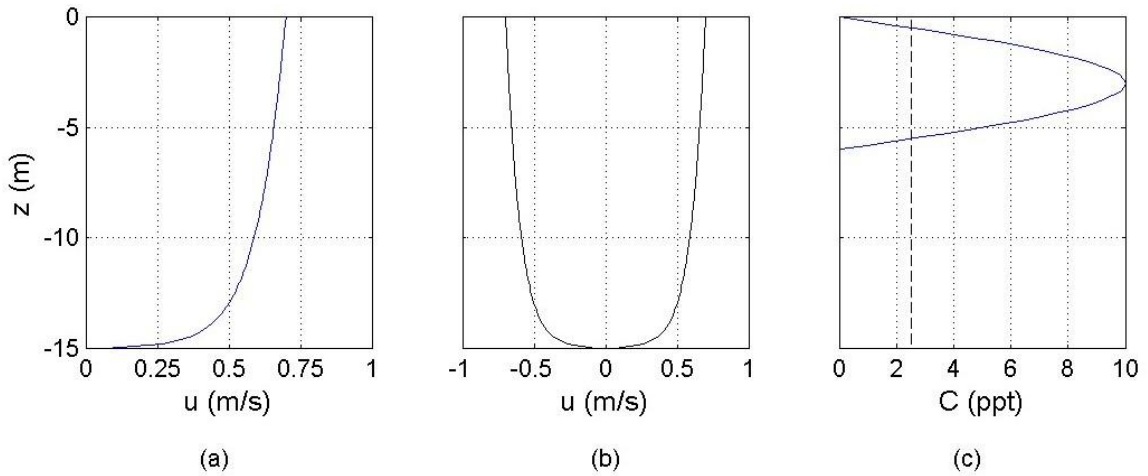


**Figure 3.3.** Fully developed velocity profiles and concentration profiles for the unstratified base case, (a) uni-directional flow; (b) oscillatory flow; and (c) initial concentration profile: solid line, and final concentration profile: dashed line.

Figure 3.4 shows the concentration distributions of  $C$  for the continuously stratified case in a uni-directional channel flow. The initial passive scalar plume  $C$  with a maximum concentration of 10 ppt was released near the top (free surface), near the middle, and close to the bed of the channel in a fully developed channel flow as shown in

figure 3.4(a) – (c). For each of the three different cases, each of the four formulations of  $Pr_t$  was implemented to predict the vertical mixing of  $C$ . For this case, the MA model predicted the maximum amount of turbulent mixing of  $C$  (see figure 3.4(g) – (i)) while the KM model predicted the minimum amount of turbulent mixing of  $C$  as shown in figure 3.4(m) – (o). The final concentration profiles for the PGT model are shown in figure 3.4(d) – (f) and those for the VS model are given in figure 3.4(j) – (l). The  $Ri$  values close to the free surface get quite large for this linearly stratified case and hence the models of both VS and KM predict the least amount of scalar mixing as can be seen from the concentration gradients at the free surface in figures 3.4(j) – (l) and 3.4(m) – (o) respectively.

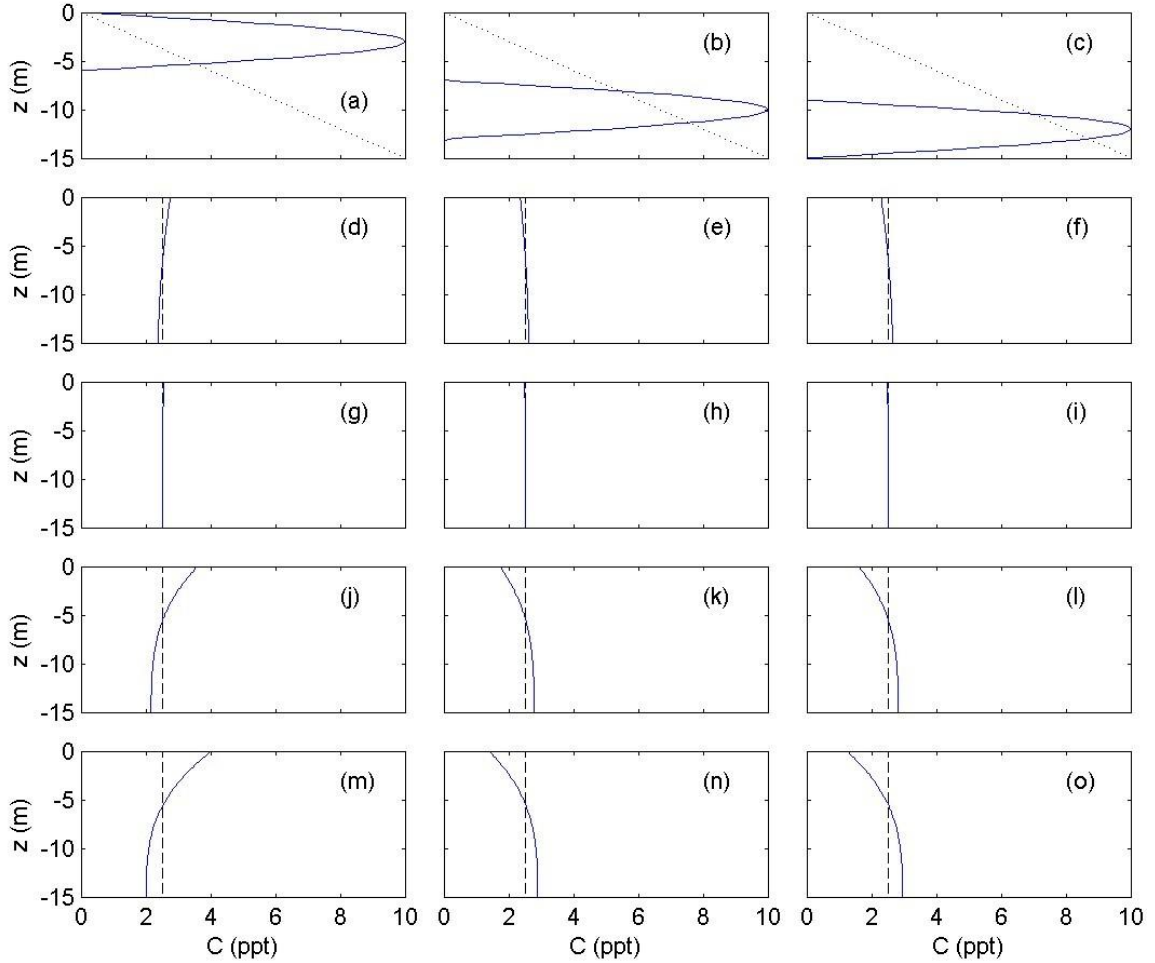


**Figure 3.4.** Concentration profiles for a passive scalar  $C$  in a continuously stratified uni-directional channel flow. Subplots (a) – (c) show the initial distribution of the passive scalar plume. Final concentration profiles are shown in subplots (d) – (f) using the PGT model; subplots (g) – (i) using the MA model; subplots (j) – (l) using the VS model; and subplots (m) – (o) using the KM model, respectively. Also superimposed on subplots (d) – (o) is the final profile for the unstratified case.

Figure 3.5 shows the concentration distributions for the two-layered stratified case (with a pycnocline) in a uni-directional channel flow. Again, the passive scalar plume  $C$  with a maximum concentration of 10 ppt was released at the same three locations as for the continuously stratified case shown in figure 3.4. For this case, the MA model for  $Pr_t$  once again mixed out the initial plume the quickest over the depth of the channel as

shown in figure 3.5(g) – (i). At the same corresponding time, the model of PGT had also almost completely mixed out the initial profile as can be seen in figure 3.5(d) – (f). The final concentration profiles using the VS model are also almost completely mixed out and so were the final concentration profiles from the KM model, but the KM model predicted the least amount of mixing of  $C$  among the four models at the same corresponding time over the depth of the flow.

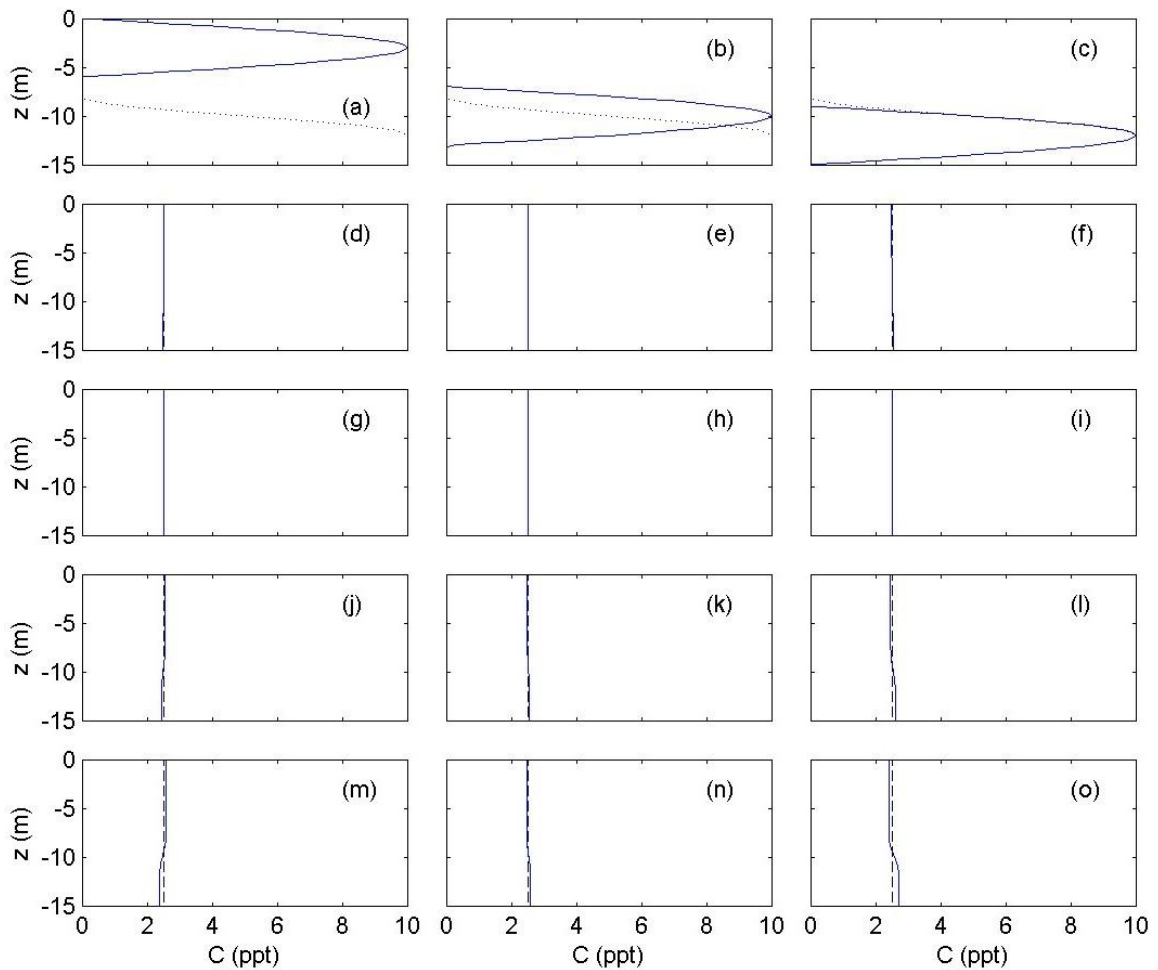


**Figure 3.5.** Concentration profiles for a passive scalar  $C$  in a two-layered stratified unidirectional channel flow. Subplots (a) – (c) show the initial distribution of the passive scalar plume. Final concentration profiles are shown in subplots (d) – (f) using the PGT model; subplots (g) – (i) using the MA model; subplots (j) – (l) using the VS model; and subplots (m) – (o) using the KM model, respectively. Also superimposed on subplots (d) – (o) is the final profile for the unstratified case.

The same conditions and models were then tested for the case of a tidally-driven periodic channel flow in which the velocity field changes direction as a function of time (see the velocity profile shown in figures 3.1(a) and 3.3(b)). For this oscillatory flow case, the turbulence grows and decays with the phase of the tide and hence stratification effects are expected to be more dominant for this flow condition compared with the uni-directional flow cases shown in figures 3.4 and 3.5.

Figure 3.6 shows the results of the mixing of  $C$  for each of the four formulations of  $Pr_t$  for a continuously stratified tidally-driven flow. Figure 3.7 shows the results of the mixing of  $C$  for the two-layered stratified tidally-driven flow. For both of these cases and for all three initial release locations of the plume, the PGT model predicted the quickest turbulent mixing of  $C$  as shown in figures 6(d) – (f) and 7(d) – (f) and the KM model again predicted the slowest turbulent mixing of  $C$  (see figures 6(m) – (o) and 7(m) – (o)). The final concentration profiles from the MA model shown in figures 6(g) – (i) and 7(g) – (i) are not quite as well mixed as the profiles from the PGT model for the oscillatory flow case. This is a direct result of the increased influence of buoyancy forces over a substantial portion of the flow depth with  $Ri$  values well above the cross-over value of  $Ri = 14.9$  between these two models discussed earlier (see figure 3.2), especially for the linearly stratified case. The VS model continues to fall in between the extremes of high and low mixing as shown in figures 6(j) – (l) and 7(j) – (l) respectively. This is expected from the model behavior of  $Pr_t$  as a function of  $Ri$  as shown in figure 3.2.

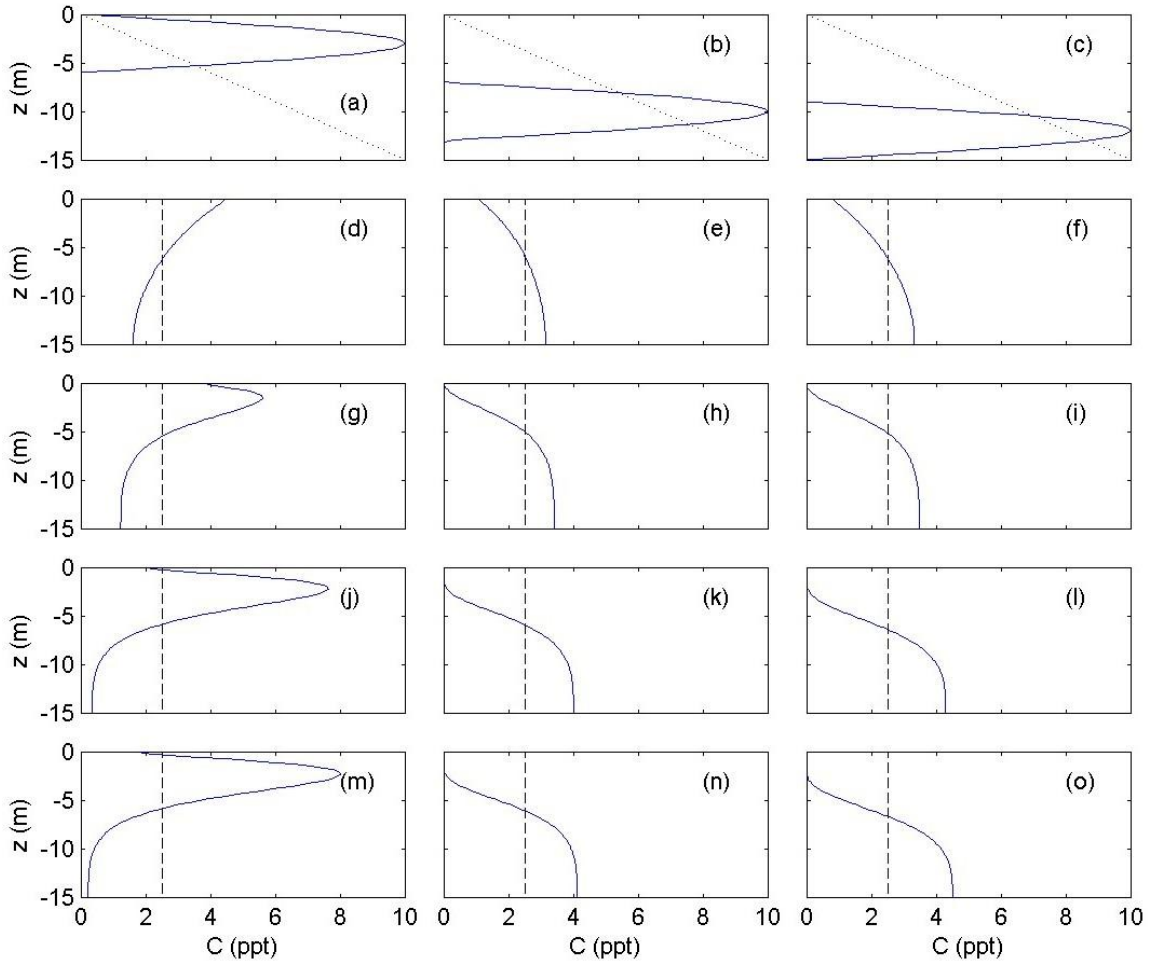


**Figure 3.6.** Concentration profiles for a passive scalar  $C$  in a continuously stratified tidally-driven channel flow. Subplots (a) – (c) show the initial distribution of the passive scalar plume. Final concentration profiles are shown in subplots (d) – (f) using the PGT model; subplots (g) – (i) using the MA model; subplots (j) – (l) using the VS model; and subplots (m) – (o) using the KM model, respectively. Also superimposed on subplots (d) – (o) is the final profile for the unstratified case.

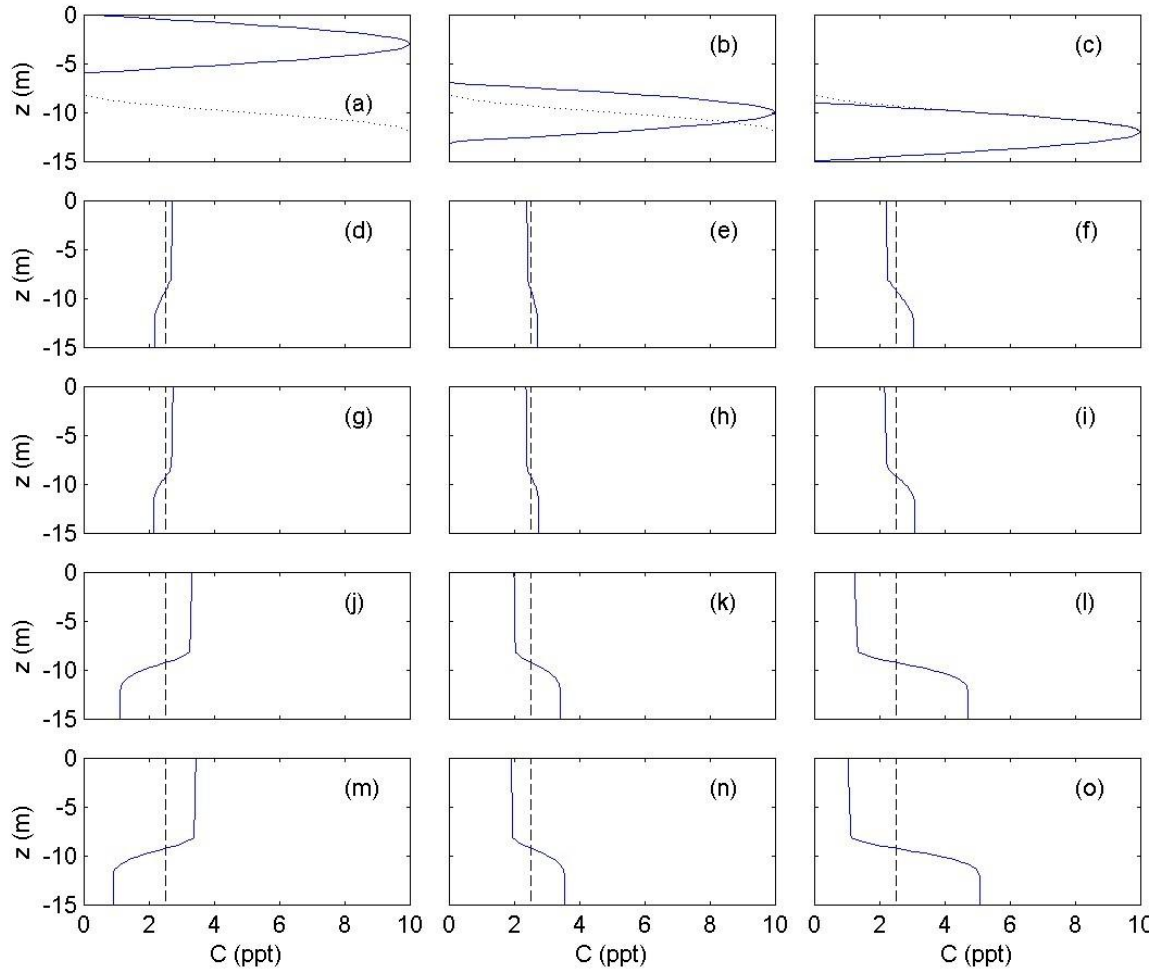


**Figure 3.7.** Concentration profiles for a passive scalar  $C$  in a two-layered stratified tidally-driven channel flow. Subplots (a) – (c) show the initial distribution of the passive scalar plume. Final concentration profiles are shown in subplots (d) – (f) using the PGT model; subplots (g) – (i) using the MA model; subplots (j) – (l) using the VS model; and subplots (m) – (o) using the KM model, respectively. Also superimposed on subplots (d) – (o) is the final profile for the unstratified case.

### 3.5 Conclusions

In this chapter, a one-dimensional vertical fluid column numerical model has been used to evaluate and compare four different parameterizations of the turbulent Prandtl number  $Pr_t$  that are used in turbulence closure models. The four parameterizations of  $Pr_t$

that are considered in this study are based on different hypotheses, observations, and numerical simulations and show considerable variability. For example, the formulation presented by VS is the only model considered here that is based on theoretical derivation and physical arguments supported by DNS data as opposed to the others, which are mainly empirically driven. The results from model-to-model comparisons using simple turbulent open-channel flow test cases highlight the effects of strong stratification in high Reynolds number flows and the impact of the different parameterizations of  $Pr_t$  on the vertical mixing of a passive scalar plume. The asymptotic behavior of  $Pr_t$  for large  $Ri$  in the PGT model allowed for a greater level of mixing than the other three models, especially for the strongly stratified oscillatory channel flow cases as shown in figures 3.6 and 3.7 respectively. On the other hand, the VS model always predicted a rate of mixing of  $C$  that was less than the models of PGT and MA, but had a mixing rate greater than the model proposed by KM.

While model-to-model comparisons alone are not sufficient in pinpointing the most appropriate model for  $Pr_t$ , they nevertheless provide valuable insight on the performance of the different parameterizations under these simple but strong test cases for scalar mixing. Given that the VS model was the only model with strong theoretical underpinning, it appears to be a promising choice but its appropriateness remains to be validated with field measurements. Furthermore, it is worth noting that this study shows how even a one-dimensional vertical fluid column model with a zero-equation turbulence closure scheme can be used to highlight the effects of stable stratification on turbulence and vertical mixing of passive scalars. In the next chapter, the study of stratified turbulence parameterizations is extended to a dynamic two-equation turbulence model.

# CHAPTER 4

## DEVELOPMENT AND TESTING OF STRATIFICATION PARAMETERS IN TWO-EQUATION TURBULENCE MODELS

### 4.1 Introduction

The selection of a basic or a comprehensive turbulence model is dependent on the underlying physics to be modeled as well as the scale and complexity of the flow type and geometry itself. While simple models can be effectively used and manipulated to fit a certain problem and yield good results, they are often not as general in their application to the many types of turbulent flows. There is a range two-equation models, including the  $k$ - $\varepsilon$  model developed by Jones and Launder (1972) and Wilcox's  $k$ - $\omega$  model (1993), which are widely used in engineering analysis and design of turbulent flows. While they may not be as accurate or computationally thorough as DNS or LES, they are suitable for catering to a wide range of turbulent flow applications and generating effective results.

In this chapter, DNS data of stably stratified homogeneous turbulence are used to study the parameters in two-equation RANS turbulence models such as the turbulent Prandtl number  $Pr_t$  and the buoyancy parameter  $C_{\varepsilon 3}$  in the standard  $k$ - $\varepsilon$  model. Both the gradient Richardson number  $Ri$  and the turbulent Froude number  $Fr_k$  are used as correlating parameters to characterize stratification in the  $k$ - $\varepsilon$  model. Modifications to the

standard  $k$ - $\varepsilon$  model based on these parameters are implemented in a one-dimensional water column model called General Ocean Turbulence Model (GOTM) and used to simulate stably stratified channel flows in which the density profiles are allowed to evolve as a function of time and as a result of the turbulent mixing and transfer of momentum. The results from numerical simulations using the modified  $k$ - $\varepsilon$  model are compared to stably stratified channel flow DNS data to assess its efficacy and determine the most appropriate parameter definitions for use in two-equation models.

## 4.2 Problem Set-Up

The test case used for the numerical simulations is that of a pressure gradient driven open-channel flow in which the density is held fixed at both the lower solid boundary and upper free surface (i.e. Dirichlet boundary conditions), again similar to the simulations and experiments done by Venayagamoorthy *et al.* (2003) and Komori *et al.* (1983). The set-up is still to some extent a simulated test case, but enforcing Dirichlet boundary conditions allows the parameters that characterize stratification to be rigorously tested in a stratified environment since in these simulations the density is allowed to evolve and mix naturally with the flow as an active scalar between the fixed boundaries. In this way, the flow is kept under stratified conditions for the duration of each of the simulations. By fixing the density at the upper and lower boundaries, the initial density profile becomes a continuously stratified profile varying with depth in the channel as shown by the blue solid line in figure 4.1. If Neumann or flux boundary conditions were instead used to define the density profile, the stratification quickly mixed out over the

depth of the channel as shown by the black dashed line in figure 4.1, thus nullifying the effects of stratification on the flow and the model parameters.

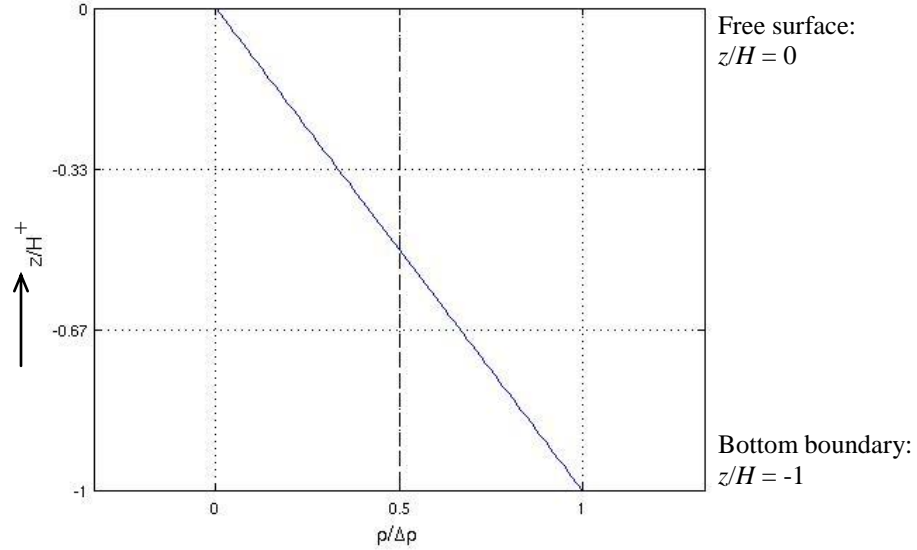


**Figure 4.1.** Density profiles: blue solid line, initial continuously stratified density profile using Dirichlet boundary conditions; black dashed line, mixed-out unstratified density profile using Neumann boundary conditions.

Before the stratified boundary conditions were imposed, the model was first allowed to spin up so as to enable the velocity field to converge to that of a fully developed, unstratified channel flow using the standard  $k-\varepsilon$  model (Venayagamoorthy *et al.* 2003). This was done to ensure that both the velocity and density fields would eventually converge on a solution, even after the stratification was imposed on the developed unstratified flow. Because density is an active scalar that influences development of the flow, density and momentum are coupled and affect one another in stratified flows. In a numerical simulation, the flow will hardly develop towards a steady-state solution for a given pressure gradient that drives the flow if the stratification is imposed using Dirichlet boundary conditions before the velocity is fully developed. Thus,

the initial stratification profile depicted in figure 4.1 was imposed on the fully developed unstratified channel flow to most realistically simulate a fully developed stratified channel flow case.

The simulations were conducted at friction Reynolds numbers of  $Re_\tau = 550$  and  $590$  and friction Richardson numbers of  $Ri_\tau = 0$  (unstratified) and  $60$ . The results were then compared to stably stratified channel flow DNS data computed by García-Villalba & del Álamo (2009) and Moser *et al.* (1999). A flow depth of  $0.2$  m in a smooth channel was also used to define the physical characteristics of the flow for each of the different test cases.

### **4.3 Numerical Modeling**

The numerical simulations were carried out using a one-dimensional water column model called General Ocean Turbulence Model (GOTM) developed by Burchard *et al.* (1999) and used for a wide range of applications in geophysical turbulence modeling. The main function of GOTM is to compute solutions for the one-dimensional transport equations of momentum, salt, and heat by solving the RANS equations via turbulence models for the turbulent fluxes of these quantities. GOTM contains several well-tested turbulence models (e.g. the  $k$ - $\epsilon$  model and the Mellor and Yamada model) that can be coupled with different combinations of turbulence parameters or stability functions to model vertical mixing in natural waters. GOTM's built-in turbulence models range from simple prescribed expressions for the momentum and scalar turbulent diffusivities to complex Reynolds-stress models, which solve several different transport

equations that model the turbulent fluxes. Although GOTM is strictly a one-dimensional code, it has been designed in a way that it can easily be coupled to a two- or three-dimensional model and used as a module for computing the vertical components of turbulent mixing (Umlauf *et al.* 2007).

GOTM is designed in a modular structure, which in addition to allowing easy integration into a more complete model, facilitates refinements and/or the introduction of new models and turbulent parameterizations. Figure 4.2 shows the modular format of GOTM and its functioning (taken from the GOTM website, [www.gotm.net](http://www.gotm.net)). Each of the modules or subroutines in GOTM is written in the FORTRAN95 language and the source code is freely available from the GOTM website, [www.gotm.net](http://www.gotm.net).

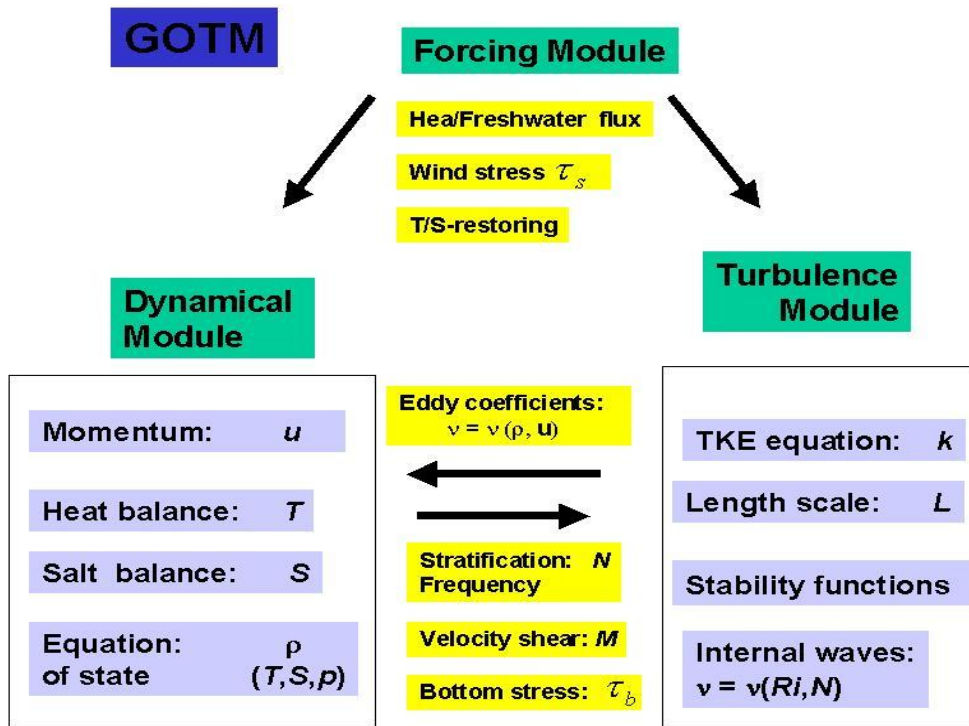


**Figure 4.2.** Modular structure of GOTM

In addition to the FORTRAN95 subroutines that are called to execute the algorithm, various input files are used to read in the different parameters specified for the numerical model. These include discretization and run-time parameters, turbulence model parameters, external observations, and data output information. Using a make utility, an executable file is built from the GOTM source code which can then be accessed from within a test case folder to run the GOTM program. Finally, GOTM outputs one-dimensional flow and turbulence results of the simulation along with any other user-specified and programmed results according to the specified file format (e.g. NetCDF or ASCII) and location. Default simulation results output by GOTM include mean flow velocity  $\bar{u}$ , buoyancy  $B$ , turbulent momentum diffusivity  $\nu_t$ , heat and scalar diffusivity  $\Gamma_t$ , turbulent kinetic energy  $k$ , and turbulent kinetic energy dissipation rate  $\varepsilon$ .

GOTM uses a finite volume method on a staggered grid for the spatial discretization of the water column. The water column is divided into a finite number of layers  $N_i$  of thickness  $h_i$  specified by the user in one of the input files. The user is also able to specify a grid of uniform spacing with  $N_i$  layers of equal thickness or one with grid zooming for thinner layers and more grid points near boundaries. A staggered grid means that the values for the mean flow quantities (e.g. mean flow velocity, temperature, and salinity) are located at the center of each interval or cell and the values for the turbulent quantities (e.g. turbulent kinetic energy, turbulent kinetic energy dissipation rate, and turbulent diffusivities) are calculated at the interfaces of the cells. Since the grid contains information at every 1/2 index, the 1/2 indices must be shifted so that they can be programmed into a computer generated grid. GOTM defines the indexing such that the

top interval of a given cell takes the same index as that cell. The spatial organization and indexing of the numerical grid is shown in figure 4.3 (Umlauf *et al.* 2007).

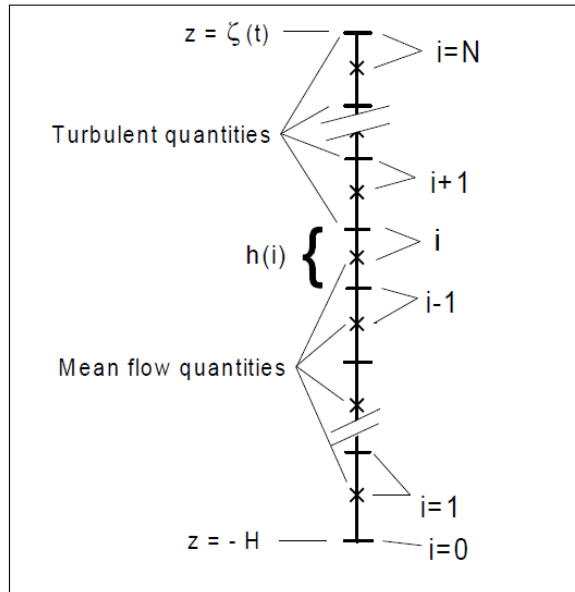


**Figure 4.3.** Spatial organization and indexing of the numerical grid in GOTM

GOTM also uses an equidistant time discretization scheme (similar to that of the  $\theta$ -method used in chapter three) based on the current time step  $t = T$  and the next time step  $t = T + \Delta t$  or fractions thereof. The stability of the time discretization scheme is not limited by Courant numbers (i.e. grid or time step size) because vertical advection is assumed to be zero and vertical diffusion is treated implicitly. Analogous to the  $\theta$ -method, GOTM uses an implicitness parameter  $\sigma$  to define a semi-implicit time level at which solutions are computed on the numerical grid as shown in figure 4.4 (Umlauf *et al.* 2007).

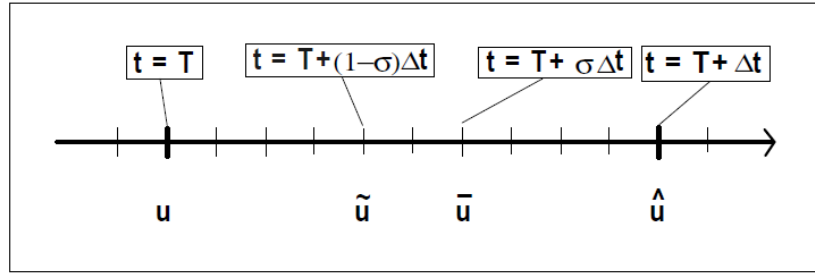


**Figure 4.4.** Temporal organization and indexing of the numerical grid in GOTM, shown with an implicitness parameter  $\sigma = 0.6$ .

GOTM includes a wide range of turbulence models, of which at least one member of every significant model family can be found (e.g. empirical models, energy models, two-equation models, algebraic stress models,  $K$ -profile parameterizations, etc.). The  $k$ - $\varepsilon$  model is an example of a two-equation RANS turbulence model in which model transport equations are solved for turbulent quantities that characterize the flow. The aim of RANS models is to calculate an eddy viscosity  $\nu_t$  so that the Reynolds-averaged governing equations given in equation (2.8) can be closed via a model given by the turbulent-viscosity hypothesis in equation (2.11). The  $k$ - $\varepsilon$  model was the first to be used in applied computational fluid dynamics and remains one of the most popular RANS turbulence models for engineering and geophysical flow calculations (Durbin & Pettersson Reif 2001). Because of its popularity and effectiveness in modeling simple unstratified shear flows, the  $k$ - $\varepsilon$  model was selected in this study to implement and test new parameterizations for  $Pr_t$  and  $C_{\varepsilon 3}$  for a stably stratified channel flow within the framework of the GOTM code.

It is well known that turbulent flows contain a wide range of scales of motion and structures. In 1941 Andrey Nikolaevich Kolmogorov first hypothesized that the largest

turbulent eddies in a flow characterized by a lengthscale  $L$  contain most of the turbulent kinetic energy  $k$ . This energy is then transferred to eddies of smaller and smaller lengthscales until the energy is dissipated into heat by viscous action (determined by the molecular momentum diffusivity or viscosity of the fluid  $\nu$ ) at the smallest scales of motion. The rate at which energy is transferred and dissipated in the flow is called the turbulent kinetic energy dissipation rate  $\varepsilon$  and is a key parameter in analyzing non-dimensional variables in turbulent flows. However, it should be noted that it is not possible to form a non-dimensional parameter from only  $\varepsilon$  and  $\nu$ . Thus, Kolmogorov also hypothesized that in every turbulent flow the statistics of the motions of scale in the range in which the overall lengthscale  $L$  is much greater than the smallest scales of motion have a universal form that is uniquely determined by  $\varepsilon$  and is independent of  $\nu$  for sufficiently high Reynolds numbers. These two hypotheses have since become the central hypotheses in turbulence theory (Pope 2000).

Using this knowledge reasoned by Kolmogorov, the two turbulence quantities  $k$  and  $\varepsilon$  that are assumed to characterize the local state of turbulence can be used to form a turbulence lengthscale ( $L = k^{3/2}/\varepsilon$ ), a turbulence timescale ( $T_L = k/\varepsilon$ ), and a quantity of dimension  $\nu_t$  ( $k^2/\varepsilon$ ). Model transport equations in the form of partial differential equations are defined to solve for the quantities  $k$  and  $\varepsilon$  and attain closure to the set of governing Reynolds-averaged equations. In the standard  $k$ - $\varepsilon$  model developed by Jones and Launder (1972) the equation for the turbulent kinetic energy  $k$  can be written as

$$\frac{Dk}{Dt} = P - \varepsilon - B + D_k. \quad (4.1)$$

$P$  is defined as the production rate of turbulent kinetic energy due to shear. For simple shear flows where mean velocity varies in one direction (e.g. fully developed open-channel flow)  $P$  can be estimated as

$$P = -\overline{u'w'S} . \quad (4.2)$$

The standard form of the  $k$ - $\varepsilon$  model allows for some accounting of buoyancy effects through the buoyancy flux term  $B$  in equation (4.1), where  $B$  is given as

$$B = -\frac{g}{\rho} \overline{\rho'w'} . \quad (4.3)$$

The sign of  $B$  depends on the static stability (i.e. stratification) of the flow. For stably stratified flows, the sign of  $B$  will be negative as restoring buoyant forces oppose momentum and cause a dissipation or “negative production” of turbulent kinetic energy in the flow. The opposite is true for unstably stratified flow conditions in which the overturning buoyant forces cause an additional production of turbulent kinetic energy, which in turn enhances turbulent mixing. Finally,  $D_k$  is the diffusion of turbulent kinetic energy, modeled using the gradient-diffusion hypothesis as

$$D_k = \frac{\partial}{\partial z} \left( \frac{v_t}{\sigma_k} \frac{\partial k}{\partial z} \right), \quad (4.4)$$

where  $\sigma_k$  is a turbulent Prandtl number for kinetic energy (see table 4.1).

The equation for the rate of dissipation of turbulent kinetic energy  $\varepsilon$  utilized by the  $k$ - $\varepsilon$  model is written as

$$\frac{D\varepsilon}{Dt} = C_{\varepsilon 1} \frac{P\varepsilon}{k} - C_{\varepsilon 2} \frac{\varepsilon^2}{k} - C_{\varepsilon 3} \frac{B\varepsilon}{k} + D_{\varepsilon}. \quad (4.5)$$

$D_{\varepsilon}$  is a diffusion transport term, analogous to  $D_k$  in that it is also modeled using the gradient-diffusion hypothesis as

$$D_{\varepsilon} = \frac{\partial}{\partial z} \left( \frac{\nu_t}{\sigma_{\varepsilon}} \frac{\partial \varepsilon}{\partial z} \right). \quad (4.6)$$

where  $\sigma_{\varepsilon}$  is a turbulent Prandtl number for dissipation. The coefficients in equation (4.5)  $C_{\varepsilon 1}$  and  $C_{\varepsilon 2}$  are adopted empirical constants in the standard form of the model (see table 4.1).

Using equations (4.1) and (4.5) to compute  $k$  and  $\varepsilon$ , the eddy viscosity  $\nu_t$  can then be defined as a dimensionally consistent function of the two turbulence parameters as

$$\nu_t = C_{\mu} \frac{k^2}{\varepsilon}, \quad (4.7)$$

where  $C_{\mu}$  is another empirical parameter. Again the eddy diffusivity  $\Gamma_t$  is related to the eddy viscosity  $\nu_t$  via the turbulent Prandtl number  $Pr_t$  and with a given a formulation of  $Pr_t$  can be computed as

$$\Gamma_t = \frac{\nu_t}{Pr_t}. \quad (4.8)$$

The values of each of the empirical parameters in equations (4.4) – (4.7), assumed to be constants in the standard  $k$ - $\varepsilon$  model, are given in table 4.1 (Rodi 1987).

**Table 4.1.** Empirical constant values for the standard  $k$ - $\varepsilon$  model

$C_\mu$	$C_{\varepsilon 1}$	$C_{\varepsilon 2}$	$\sigma_k$	$\sigma_\varepsilon$
0.09	1.44	1.92	1.0	1.3

There is no clear consensus on values and/or formulations of  $Pr_t$  and  $C_{\varepsilon 3}$  for stratified flows in the turbulence modeling community. Numerically generated results for stratified flows have been shown to be very sensitive to these two parameters. Constant values as well as numerous models of  $Pr_t$  as a function of  $Ri$  for stratified flows have been presented and discussed in chapter three. There are nearly as many proposed parameterizations for  $C_{\varepsilon 3}$  as there are for  $Pr_t$ . Many tests have even shown that the value of  $C_{\varepsilon 3}$  depends on the type of stratification present in a given flow. Rodi (1987) shows that for unstably stratified flows where  $B$  is an energy source term  $C_{\varepsilon 3}$  should be approximately equal to 1, and for stably stratified flows  $C_{\varepsilon 3}$  should take a value between 0 and 0.2. Other parameterizations by Baum and Caponi (1992) and Burchard and Baumert (1995) propose values of  $C_{\varepsilon 3} = 1.14$  and  $C_{\varepsilon 3} < 0$ , respectively. Still others have reasoned that the buoyancy flux term  $B$  should be treated analogous to the turbulent kinetic energy production term  $P$ , thus setting the value of  $C_{\varepsilon 3} = 1.44$ .

In addition to the many well-known and tested turbulence models, GOTM also contains a number of built-in stability functions that are computed and updated and used to calculate the turbulence closure parameters. Depending on the level and complexity of turbulence model used, these stability functions can either be constants, empirical functions, or functions of parameters characterizing the local state of turbulence. In the standard  $k$ - $\varepsilon$  model, these stability functions are the model parameters given in table 4.1 as well as  $Pr_t$  and  $C_{\varepsilon 3}$ . The version of GOTM used also has a subroutine for computing stability functions according to Munk and Anderson's (1948) model that was evaluated in chapter three. GOTM's open-source modular format allows stability functions to be modified and/or created to test different parameterizations of the stability functions. In order to rigorously test the effectiveness of the  $k$ - $\varepsilon$  model in simulating stably stratified flows and propose an efficient model, different variations of the  $k$ - $\varepsilon$  model were assessed by using different stability functions to define the turbulence parameters. The stability functions tested include the built-in standard form of the model using only the original empirical constants developed by Jones and Launder (1972), the built-in Munk and Anderson (1948) model for computing  $\nu_t$  and  $Pr_t$  as functions of  $Ri$  (see equation (3.15)), the Venayagamoorthy and Stretch (2010) model for computing  $Pr_t$  as a function of  $Ri$  (see equation (3.16)), and finally a proposed model for stably stratified flows based on  $Pr_t$  and  $C_{\varepsilon 3}$  as functions of the turbulent Froude number  $Fr_k$ . The FORTRAN95 code modules for the modified and/or created stability functions and boundary conditions used in GOTM for this study can be found in appendix B.

## 4.4 Results

The ability of each of the four tested stability functions to simulate fully developed, stably stratified turbulent channel flow was assessed using the  $k$ - $\varepsilon$  model in GOTM. DNS data of stably stratified homogeneous turbulence in channel flow at a friction Reynolds number of  $Re_\tau = 550$  and friction Richardson numbers of  $Ri_\tau = 0$  and 60 were used to validate the results computed in GOTM. The mean flow and turbulence parameters of interest that were analyzed and compared to the DNS include the mean flow velocity (non-dimensionalized as  $u/u_\tau$ ), turbulent kinetic energy (non-dimensionalized as  $k/u_\tau^2$ ), turbulent kinetic energy dissipation rate (non-dimensionalized as  $\varepsilon/(u_\tau^3 H^{-1})$ ), and density (non-dimensionalized as  $\rho/\Delta\rho$ ).

The standard  $k$ - $\varepsilon$  model used as the base case in GOTM was first calibrated and validated for an unstratified case ( $Ri_\tau = 0$ ) by simulating channel flows at  $Re_\tau = 550$  and 590 and comparing the results to DNS data computed by García-Villalba and del Álamo (2009) and Moser *et al.* (1999) respectively. It turns out that the  $k$ - $\varepsilon$  model in GOTM is very sensitive to a number of input parameters including grid size and spacing, boundary roughness, and the von Karman constant  $\kappa$  to name a few of the most relevant ones. Thus, the DNS data were used to calibrate these parameters. The unstratified cases in GOTM were run using the standard  $k$ - $\varepsilon$  model with constant stability functions given in table 4.1. For each case, the model was allowed to converge and reach a fully developed turbulent velocity profile to facilitate comparison with the DNS profiles. Figure 4.5(a) shows the fully developed velocity profile computed using the standard  $k$ - $\varepsilon$  model in GOTM versus the DNS data for a friction Reynolds number  $Re_\tau = 550$ . For the unstratified case, the

standard  $k$ - $\varepsilon$  model results for the mean velocity profile were in good agreement with the DNS data. The turbulence quantities  $k$  and  $\varepsilon$  computed by the standard  $k$ - $\varepsilon$  model were also used to validate the model with the DNS data at  $Re_\tau = 550$  as shown in figures 4.5(b) and 4.5(c) respectively. As expected, the  $k$ - $\varepsilon$  turbulence model did not capture all of the physics near the boundaries, but the agreement was generally good in modeling dynamic turbulence quantities.

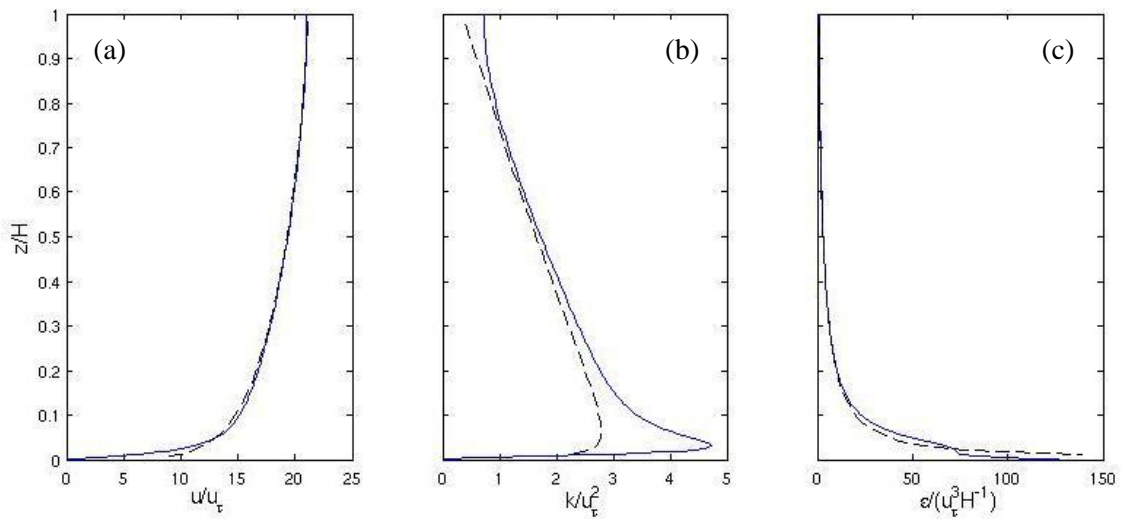


**Figure 4.5.** Distributions of (a) mean velocity  $u$ ; (b) turbulent kinetic energy  $k$ ; and (c) turbulent kinetic energy dissipation rate  $\varepsilon$  in pressure gradient driven open-channel flow at  $Re_\tau = 550$  and  $Ri_\tau = 0$ : blue solid line, DNS data (García-Villalba & del Álamo 2009); black dashed line, GOTM results (standard  $k$ - $\varepsilon$  model).

To further validate the model for the unstratified case, DNS data (from a different source) for  $Re_\tau = 590$  were also used to compare the performance of the standard  $k$ - $\varepsilon$  model in predicting the turbulent velocity profile and turbulence quantities in the channel. Figure 4.6(a) shows the fully developed velocity profile computed using the standard  $k$ - $\varepsilon$  model in GOTM versus the DNS data for a friction Reynolds number  $Re_\tau = 590$ . The model again performed well in predicting the mean velocity field in comparison to the

DNS data. Dynamic turbulence quantities were also validated versus DNS data for the case of  $Re_\tau = 590$  in figure 4.6(b) and 4.6(c). The standard  $k-\varepsilon$  model again did an excellent job of predicting the trends in the turbulence with the exception of at the channel boundaries.

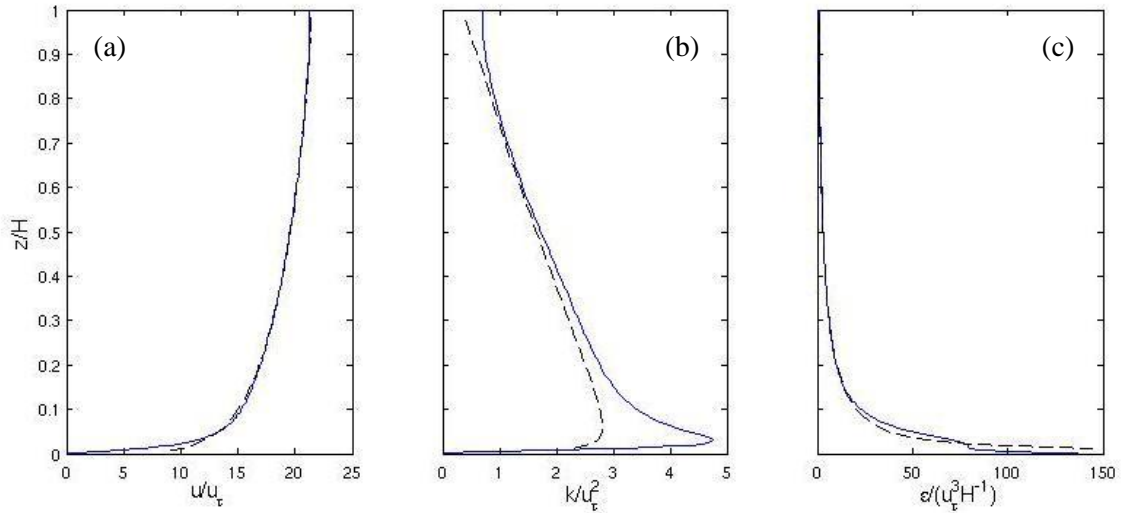


**Figure 4.6.** Distributions of (a) mean velocity  $u$ ; (b) turbulent kinetic energy  $k$ ; and (c) turbulent kinetic energy dissipation rate  $\varepsilon$  in pressure gradient driven open-channel flow at  $Re_\tau = 590$  and  $Ri_\tau = 0$ : blue solid line, DNS data (Moser *et al.* 1999); black dashed line, GOTM results (standard  $k-\varepsilon$  model).

Accepting the sufficiency of the standard  $k-\varepsilon$  model to model one-dimensional unstratified channel flow, its parameters or stability functions were modified to account for buoyancy effects and tested under stably stratified channel flow conditions. Four stability functions were assessed in their ability to predict mean velocity, density, and turbulent quantity profiles at  $Re_\tau = 550$  and  $Ri_\tau = 60$ . For each of the stratified cases, the flow was allowed to spin up and fully develop before the stratification was imposed on the channel via Dirichlet boundary conditions for the density. The flow was then allowed to converge to a steady-state solution to be evaluated against the stratified DNS results.

Figure 4.7 shows results of the  $k$ - $\varepsilon$  model with constant stability functions for  $Pr_t$ ,  $C_{\varepsilon 3}$ , and each of the other  $k$ - $\varepsilon$  model parameters in contrast to DNS data. Values of  $Pr_t = 0.71$  and  $C_{\varepsilon 3} = 1.44$  for buoyancy effects were used in addition to the standard constant values for the other parameters given in table 4.1. The constant stability functions missed the effect of stratification on the development of the mean turbulent velocity profile  $u$ , especially near the free surface in figure 4.7(a). The model did a fair job in predicting the behavior and trend of the density field  $\rho$  compared to the other models (see discussion below) in figure 4.7(b). The turbulence quantities  $k$  and  $\varepsilon$  were again adequately predicted away from the boundaries in figure 4.7(c) and 4.7(d).

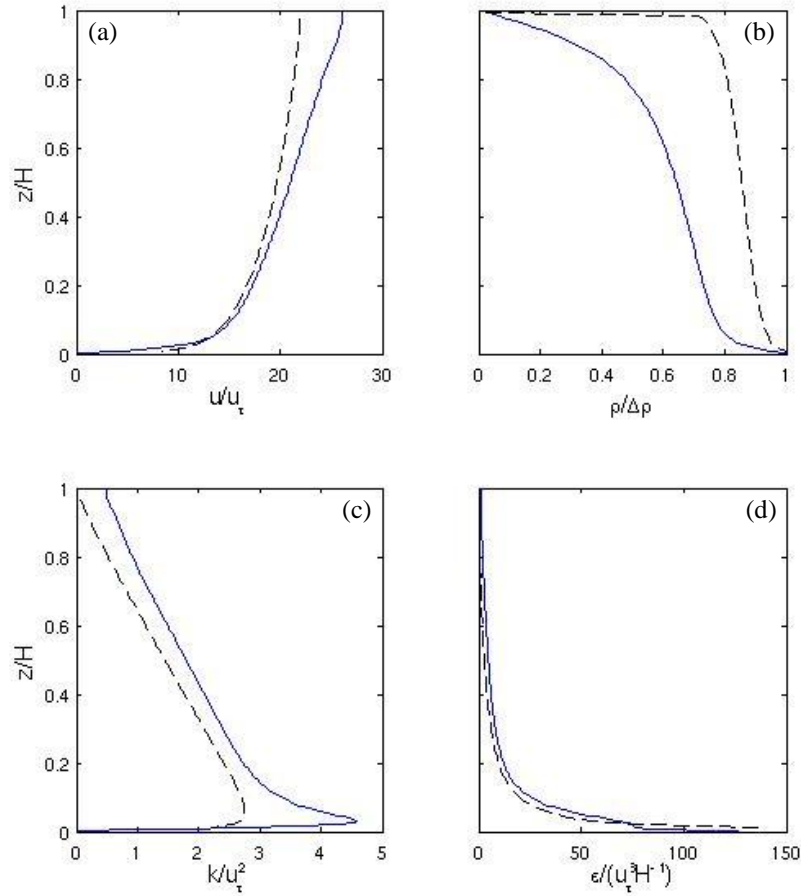


**Figure 4.7.** Distributions of (a) mean velocity  $u$ ; (b) density  $\rho$ ; (c) turbulent kinetic energy  $k$ ; and (d) turbulent kinetic energy dissipation rate  $\varepsilon$  in pressure gradient driven open-channel flow at  $Re_\tau = 550$  and  $Ri_\tau = 60$ : blue solid line, DNS data (García-Villalba & del Álamo 2009); black dashed line, GOTM results ( $k$ - $\varepsilon$  model with constant stability functions).

The same flow and stratification conditions were then used to test the Munk and Anderson (1948) and the Venayagamoorthy and Stretch (2010) stability functions in conjunction with the  $k$ - $\varepsilon$  model. These stability functions compute  $Pr_t$  as a function of the stratification in the channel with  $Ri$  and also use a constant value of  $C_{\varepsilon 3} = 1.44$  to estimate buoyancy effects. Figure 4.8 shows the predictions of the  $k$ - $\varepsilon$  model using the Munk and Anderson (1948) stability function and figure 4.9 shows the results for the  $k$ - $\varepsilon$  model using the Venayagamoorthy and Stretch (2010) stability function versus DNS results for

stably stratified turbulence. It is important to note that for both of these models,  $Ri$  did a poor job in that it over-predicted the turbulent mixing of  $\rho$  in figures 4.8(b) and 4.9(b), essentially washing out the stratification in the channel such that buoyancy effects were nullified. As a consequence, the effect of stratification on the mean velocity profiles  $u$  for each case was significantly missed near the free surface as shown in figures 4.8(a) and 4.9(a). Turbulence quantities are again shown in figures 4.8(c) – (d) and 4.9(c) – (d) for each of the models respectively.

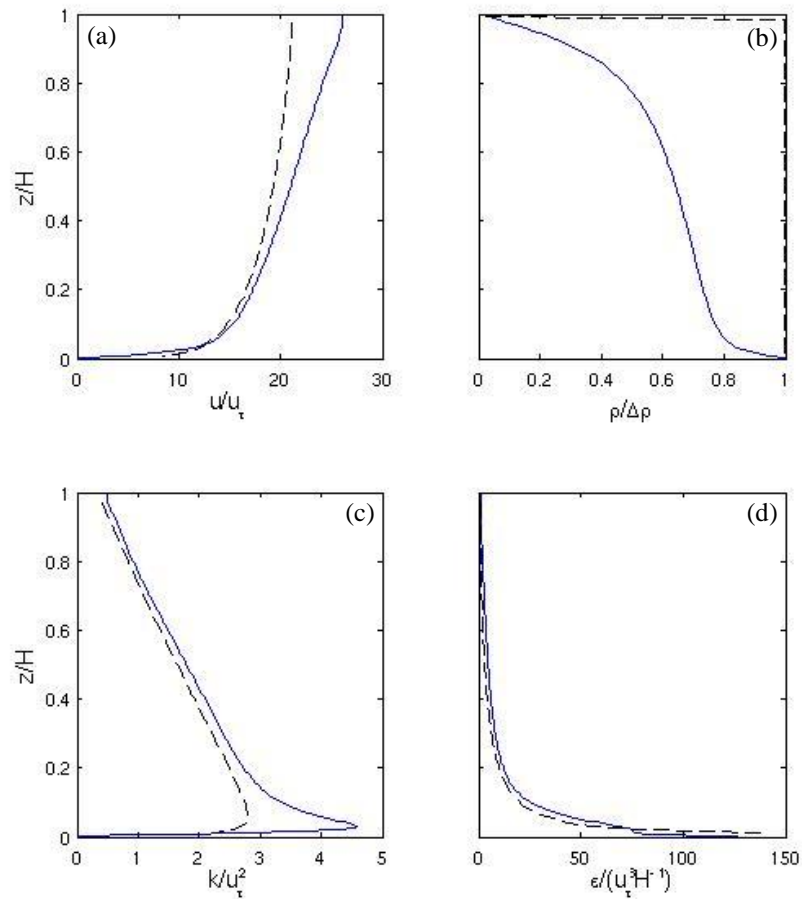


**Figure 4.8.** Distributions of (a) mean velocity  $u$ ; (b) density  $\rho$ ; (c) turbulent kinetic energy  $k$ ; and (d) turbulent kinetic energy dissipation rate  $\epsilon$  in pressure gradient driven open-channel flow at  $Re_\tau = 550$  and  $Ri_\tau = 60$ : blue solid line, DNS data (García-Villalba & del Álamo 2009); black dashed line, GOTM results ( $k$ - $\epsilon$  model with Munk and Anderson (1948) stability function).

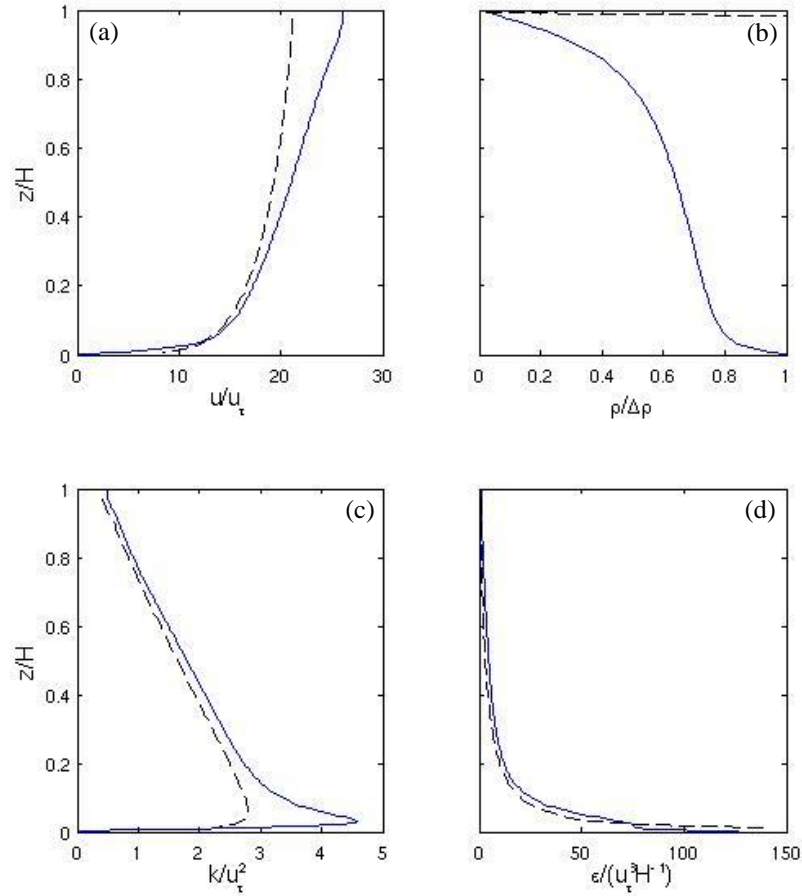


**Figure 4.9.** Distributions of (a) mean velocity  $u$ ; (b) density  $\rho$ ; (c) turbulent kinetic energy  $k$ ; and (d) turbulent kinetic energy dissipation rate  $\varepsilon$  in pressure gradient driven open-channel flow at  $Re_\tau = 550$  and  $Ri_\tau = 60$ : blue solid line, DNS data (García-Villalba & del Álamo 2009); black dashed line, GOTM results ( $k$ - $\varepsilon$  model with Venayagamoorthy and Stretch (2010) stability function).

Since  $Ri$  seems to be a poor parameter for characterizing the effects of stratified turbulence in dynamic two-equation models, it is not surprising that the  $k$ - $\varepsilon$  model with constant stability functions performed better than the Munk and Anderson (1948) and Venayagamoorthy and Stretch (2010) models at predicting the turbulent velocity profile and density field.

In lieu of the gradient Richardson number  $Ri$ , the turbulent Froude number  $Fr_k$  is a dimensionless parameter that has been suggested and used by others, including Shih *et*

*al.* (2000) and Venayagamoorthy *et al.* (2003), to describe the effects of stratification on turbulence parameters.  $Fr_k$  can be constructed by using a buoyancy lengthscale and a turbulence lengthscale. The buoyancy or Ozmidov lengthscale  $L_O$  can be defined as

$$L_O = \left( \frac{\varepsilon}{N^3} \right)^{1/2} \quad (4.9)$$

and the turbulence lengthscale  $L$  is defined as

$$L = \frac{k^{3/2}}{\varepsilon} . \quad (4.10)$$

$Fr_k$  can then be defined in terms of  $L_O$  and  $L$  as (Shih *et al.* 2000)

$$Fr_k = \left( \frac{L_O}{L} \right)^{2/3} . \quad (4.11)$$

Substituting equations (4.9) and (4.10) into equation (4.11) yields a formulation of the turbulent Froude number in terms of turbulence quantities  $k$  and  $\varepsilon$  and the stratification parameter  $N$ , written as

$$Fr_k = \frac{\varepsilon}{Nk} . \quad (4.12)$$

$Fr_k$  can also be defined in terms of two timescales as simply the ratio of the buoyancy timescale  $N^{-1}$  to the turbulence timescale  $T_L = k/\varepsilon$ , expressed by rewriting equation (4.12) in terms of  $N^{-1}$  and  $T_L$  as

$$Fr_k = \frac{1}{NT_L}. \quad (4.13)$$

It is argued by some that  $Fr_k$  is a better parameter than  $Ri$  for characterizing stratified turbulence because it is based on local turbulence quantities  $k$  and  $\varepsilon$ , whereas  $Ri$  is more of a mean property of the flow based on global, linear quantities  $N$  and  $S$ . It may be especially suitable for the  $k$ - $\varepsilon$  model because  $k$  and  $\varepsilon$  are already computed quantities.

A model for  $Pr_t$  as a function of  $Fr_k$  can be obtained by first expressing the turbulent Froude number  $Fr_k$  in terms of the gradient Richardson number  $Ri$ . Since both are functions of the Brunt-Väisälä or buoyancy frequency  $N$ , equation (2.17) for  $Ri$  can be rearranged and solved for  $N$  in terms of  $Ri$  and  $S$  as

$$N = Ri^{1/2}S. \quad (4.14)$$

Substituting equation (4.14) into equation (4.13) yields an expression for  $Fr_k$  in terms of  $Ri$ ,  $S$ , and  $T_L$  as

$$Fr_k = \frac{1}{Ri^{1/2}} \left( \frac{1}{ST_L} \right). \quad (4.15)$$

$Fr_k$  is perhaps a better parameter for stratification than  $Ri$  for dynamic two-equation models like the  $k$ - $\varepsilon$  model because of that fact that it is a function of the turbulence timescale  $T_L$ , a dynamic parameter for characterizing turbulent behavior (i.e. mixing and decay). However, since  $Fr_k$  depends on  $S$  and  $T_L$  in addition to  $Ri$ , it cannot simply be substituted directly into any of the other functions depending only on  $Ri$  without introducing the additional terms  $S$  and  $T_L$ . Thus, using DNS data of  $Pr_t$  and  $Fr_k$  and physical arguments that  $Pr_t \rightarrow Pr_{t0}$  as  $Fr_k \rightarrow \infty$  and  $Pr_t \rightarrow \infty$  as  $Fr_k \rightarrow 0$ , an expression of  $Pr_t$  as a function of  $Fr_k$  was formulated as

$$Pr_t = \zeta \exp(-\psi Fr_k) + Pr_{t0}, \quad (4.16)$$

where  $\zeta$  and  $\psi$  are empirical coefficients with values of 2.0 and 0.1 respectively.  $\zeta$  and  $\psi$  were determined using results of trial-and-error simulations in GOTM compared to DNS data of stably stratified turbulent flow. A value of  $Pr_{t0} = 1.0$  was also found to work best in predicting the mixing of momentum and density using this formulation. The function for  $Pr_t$  given in equation (4.16) is also plotted in Figure 4.10.

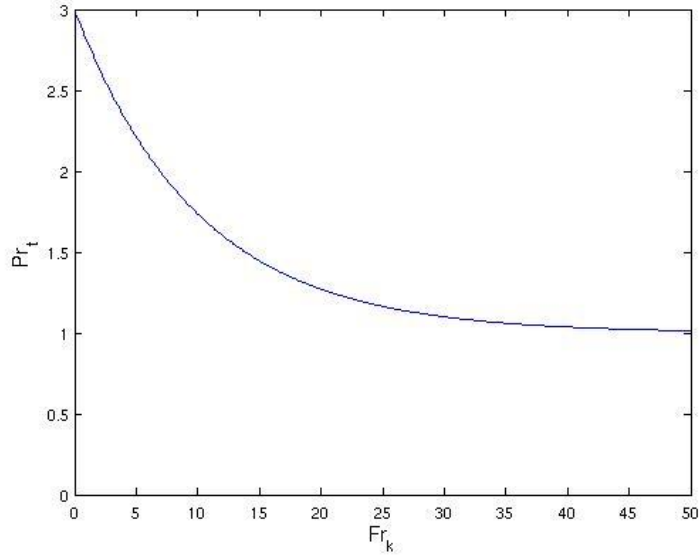


**Figure 4.10.** The turbulent Prandtl number  $Pr_t$  as a function of the turbulent Froude number  $Fr_k$  as defined in equation (4.16).

Figure 4.11 shows the results using equation (4.16) to compute  $Pr_t$  and using a constant value of  $C_{\varepsilon 3} = 1.44$ . Equation (4.16) does a significantly better job at predicting the stratified density profile in figure 4.11(b) as compared to the formulations of  $Pr_t$  that are functions of  $Ri$ . However, the model for this case still was not able to compute the correct trend in the mean velocity profile at the free surface as shown in figure 4.11(a). The results for  $k$  and  $\varepsilon$  computed using equation (4.16) are given in figures 4.11(c) and 4.11(d) respectively.

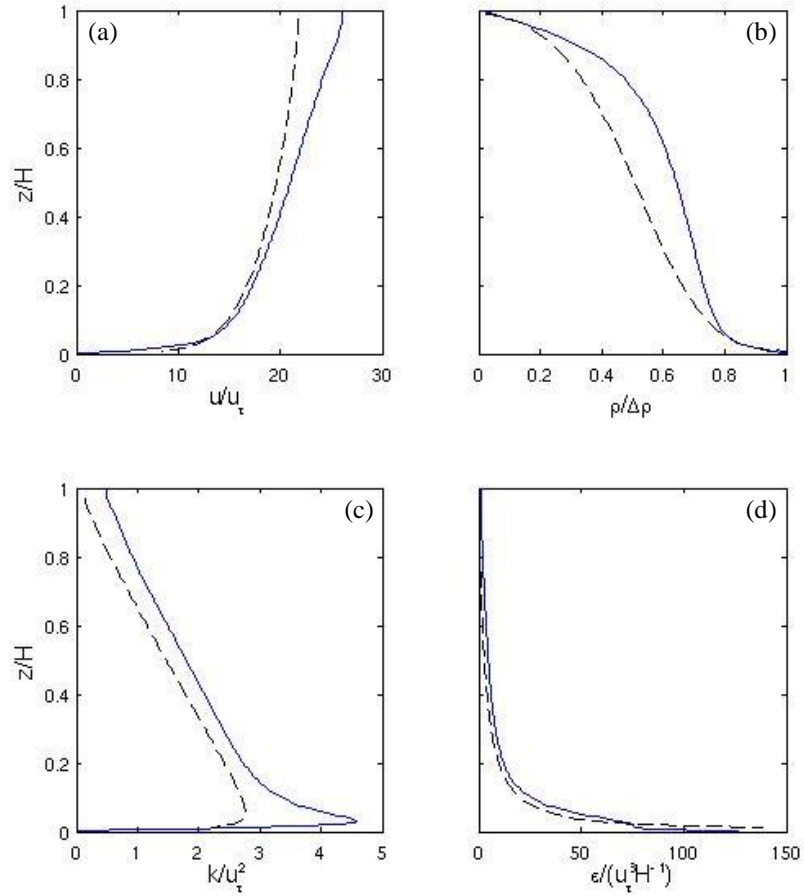


**Figure 4.11.** Distributions of (a) mean velocity  $u$ ; (b) density  $\rho$ ; (c) turbulent kinetic energy  $k$ ; and (d) turbulent kinetic energy dissipation rate  $\varepsilon$  in pressure gradient driven open-channel flow at  $Re_\tau = 550$  and  $Ri_\tau = 60$ : blue solid line, DNS data (García-Villalba & del Álamo 2009); black dashed line, GOTM results ( $k$ - $\varepsilon$  model with  $Pr_t = f(Fr_k)$  and  $C_{\varepsilon 3} = 1.44$ ).

To further adapt the  $k$ - $\varepsilon$  stability functions' ability to model stratified turbulence, the buoyancy parameter  $C_{\varepsilon 3}$  was also defined as a function of  $Fr_k$ . Again, using arguments that  $C_{\varepsilon 3} \rightarrow C_{\varepsilon 3,0}$  as  $Fr_k \rightarrow 0$  and  $C_{\varepsilon 3} \rightarrow 0$  as  $Fr_k \rightarrow \infty$  as well as trial-and-error simulations in GOTM,  $C_{\varepsilon 3}$  can be expressed in terms of  $Fr_k$  as

$$C_{\varepsilon 3} = C_{\varepsilon 3,0} \exp(-Fr_k), \quad (4.17)$$

where  $C_{\epsilon 3,0}$  is the maximum value of the buoyancy parameter  $C_{\epsilon 3}$ , computed as  $C_{\epsilon 3,0} \approx 0.48$  by multiplying the mixing efficiency  $\Gamma_{\infty} \approx 1/3$  (see chapter three) by the production parameter  $C_{\epsilon 1} = 1.44$  (see table 4.1). Figure 4.12 shows the function for  $C_{\epsilon 3}$  given in equation (4.17), non-dimensionalized as  $C_{\epsilon 3}/C_{\epsilon 3,0}$ .

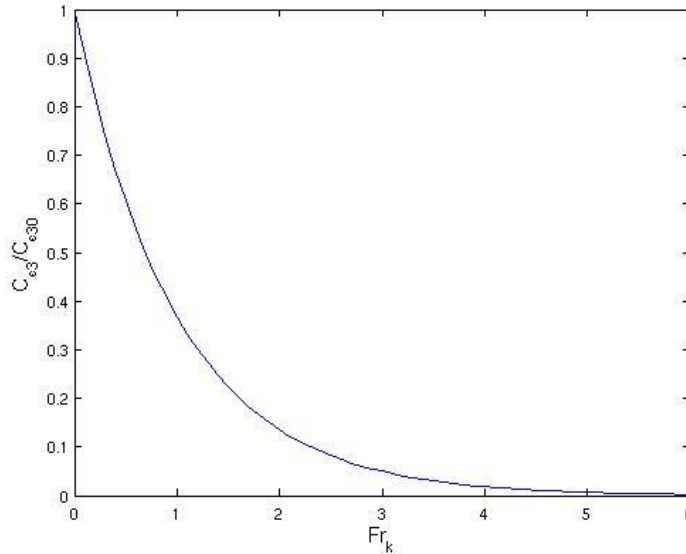


**Figure 4.12.** The buoyancy parameter  $C_{\epsilon 3}$  as a function of the turbulent Froude number  $Fr_k$  as defined in equation (4.17).

Figure 4.13 shows results using the  $k$ - $\epsilon$  model with stability functions for  $Pr_t$  and  $C_{\epsilon 3}$  defined using equations (4.16) and (4.17) respectively. By defining both  $Pr_t$  and  $C_{\epsilon 3}$  as functions of the turbulent Froude number, the model was able to more closely match the mean velocity profile in figure 4.13(a) while providing excellent predictions of the density profile in figure 4.13(b) and the turbulent quantities  $k$  and  $\epsilon$  in figures 4.13(c) and 4.13(d) respectively at  $Re_{\tau} = 550$  and  $Ri_{\tau} = 60$ .

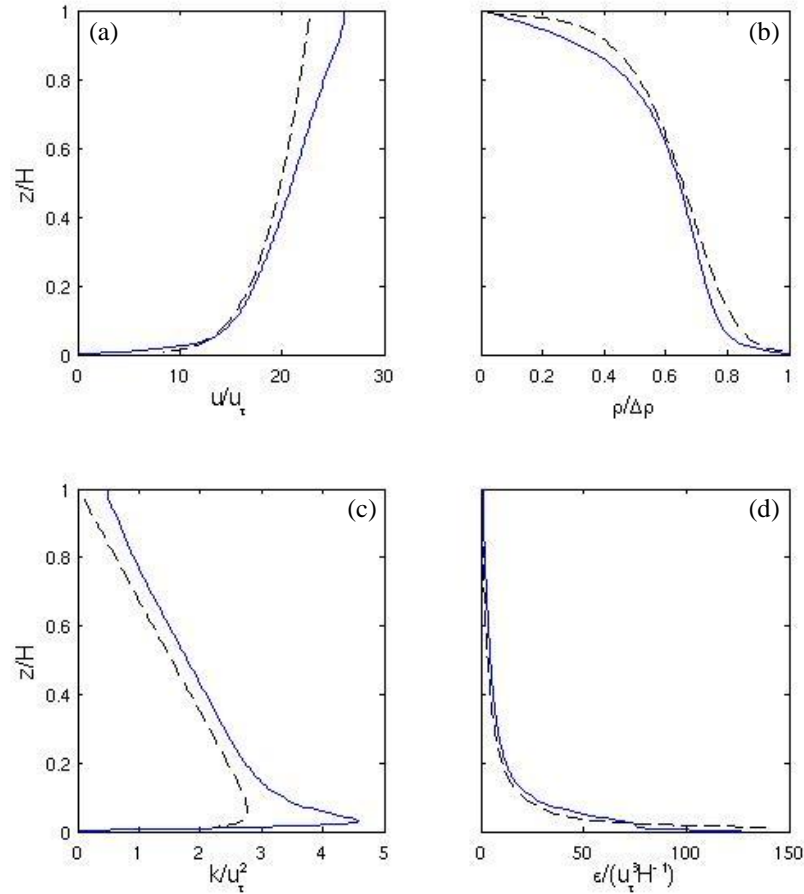


**Figure 4.13.** Distributions of (a) mean velocity  $u$ ; (b) density  $\rho$ ; (c) turbulent kinetic energy  $k$ ; and (d) turbulent kinetic energy dissipation rate  $\varepsilon$  in pressure gradient driven open-channel flow at  $Re_\tau = 550$  and  $Ri_\tau = 60$ : blue solid line, DNS data (García-Villalba & del Álamo 2009); black dashed line, GOTM results ( $k$ - $\varepsilon$  model with  $Pr_t = f(Fr_k)$  and  $C_{\varepsilon 3} = f(Fr_k)$ ).

## 4.5 Conclusions

In this chapter, one-dimensional stratified channel flow simulations using the  $k$ - $\varepsilon$  model have been used to test different formulations of the turbulent Prandtl number  $Pr_t$  and the buoyancy parameter  $C_{\varepsilon 3}$ . The results show that stratified turbulence models are very sensitive to changes in the formulation of these two parameters. Analysis of the results have shown that  $Ri$  may not be the best parameter to characterize stratification in

dynamic two-equation models and that  $Fr_k$  may be a more appropriate model parameter to represent turbulent behavior in stratified flows. The parameterizations for  $Pr_t$  and  $C_{\varepsilon 3}$  given in equations (4.16) and (4.17) respectively give good results for moderately stratified turbulence ( $Re_\tau = 550$  and  $Ri_\tau = 60$ ) and provide an initial framework for defining these parameters in a general and useful form. However, it remains to be seen how these functions will perform at higher levels of turbulence and stratification. RANS modeling is still the most practical and widely-used way to simulate turbulent flows and there still exists great motivation and potential to improve upon these and other RANS parameterizations to accurately capture the flow physics at a reasonable time and computational cost for an increasing range of engineering applications.

## CHAPTER 5

### SUMMARY AND CONCLUSIONS

#### 5.1 Summary

Buoyancy forces in stratified environmental flows have been shown to have a substantial effect on turbulent flow development and mixing. In stably stratified flows, buoyancy opposes momentum and the result is a reduction in the turbulent kinetic energy and a suppression of flow parameters that describe the vertical mixing and diffusion of momentum and scalars. Numerically modeling stratified turbulence in order to predict and analyze flow behavior is challenging due to the fact the density transport and momentum equations are inherently coupled. Therefore the density becomes an active scalar and influences the evolution of the flow.

In chapter three, one-dimensional channel flow with a zero-equation turbulence model was used to evaluate and compare four different formulations of the turbulent Prandtl number  $Pr_t$  in the presence of strong stable stratification in highly turbulent flows. A somewhat arbitrary but strong test case was used in that the density stratification was held fixed in the channel in order to rigorously test and study the effects of stable stratification on turbulent flow development and mixing. The mixing rates of a passive scalar plume  $C$  for each of the four models were compared first to the base case of

unstratified turbulent mixing and then relative to each other to assess the performance of each parameterization. Each model for  $Pr_t$  was tested under a variety of channel flow conditions representing practical flows encountered in engineering and in the environment, including uni-directional and oscillatory flows and continuous and two-layer stable density stratification. In addition to the numeric results generated by the model, the basis underlying the formulation of each model was used to consider which of the formulations of  $Pr_t$  might best represent and model the physics of stratified turbulence.

In chapter four, the  $k$ - $\varepsilon$  turbulence model was used within the framework of General Ocean Turbulence Model (GOTM), an open-source, one-dimensional water column model, to modify and test turbulence parameters in stratified channel flow using the dynamic two-equation  $k$ - $\varepsilon$  model. The problem set-up and definition was also more complete in that the density field was held fixed only at the boundaries to ensure that the stratification was not completely washed out, yet could still interact with the flow and mix between the boundaries as an active scalar. The parameters or stability functions of interest again included  $Pr_t$  as well as the buoyancy parameter  $C_{\varepsilon 3}$  in the  $k$ - $\varepsilon$  model. The  $k$ - $\varepsilon$  model in GOTM was first calibrated and validated with unstratified DNS turbulent channel flow data. Using GOTM's open-source modular format, these stability functions were then modified or created and tested under stratified conditions according to existing models including the built-in standard form of the  $k$ - $\varepsilon$  model with constant stability functions developed by Jones and Launder (1972), the built-in Munk and Anderson (1948) model, the Venayagamoorthy and Stretch (2010) model, and finally a proposed model based on parameterizations of  $Pr_t$  and  $C_{\varepsilon 3}$  as functions of the turbulent Froude

number  $Fr_k$ . The accuracy of each of the models was assessed using DNS data of stratified turbulent channel flow.

## 5.2 Conclusions

In chapter three, the different predictions yielded by each of the models tested show the importance of accurately modeling  $Pr_t$  in order to reasonably predict scalar mixing and dispersion. In addition to consistently predicting vertical mixing of a passive scalar plume that was neither the most nor the least in any of the flow scenarios, the model formulation for  $Pr_t$  of Venayagamoorthy and Stretch (2010) was the only model considered based on theoretical derivation and physical arguments supported by DNS data as opposed to purely empirical formulation. Although it still remains to be validated with field or lab data, the Venayagamoorthy and Stretch (2010) model proves to be a good choice for use in simple shear flow applications with a zero-equation turbulence model. The results of this study have also shown how even a one-dimensional vertical fluid column formulation with a zero-equation turbulence model can be effectively used as a modeling tool that is easy to implement and computationally economical to provide insightful results into the physics of turbulence and stratification.

The results of chapter four emphasized the sensitivity of turbulent parameters to the effects of stratification, namely  $Pr_t$  and  $C_{\epsilon 3}$ . The formulation of these parameters as functions of the gradient Richardson number  $Ri$  did not perform as well in a dynamic two-equation model setting as they did in a zero-equation model, leading to the conclusion that perhaps another parameter is better suited to characterize the effects of

stratification than  $Ri$ . In preliminary tests, the model parameter  $Fr_k$  was used to define  $Pr_t$  and  $C_{\varepsilon 3}$  and provided results that reasonably matched the DNS data results for mixing and transport of momentum and density.  $Fr_k$  is a better parameter because it is a dynamic function of the turbulence quantities  $k$  (turbulent kinetic energy) and  $\varepsilon$  (turbulent kinetic energy dissipation rate), which are local quantities characterizing the state of turbulence in the flow as opposed to  $Ri$ , which is a parameter based on global mean flow properties.  $Fr_k$  is also a nice choice because it does not require the specification of any extra terms to close the model in the many popular dynamic two-equation models equations that utilize  $k$  and  $\varepsilon$ .

### 5.3 Further Work

A natural extension of this study is to continue the development and refinement of the stability functions  $Pr_t$  and  $C_{\varepsilon 3}$  using  $Fr_k$  or other dynamic parameters that account for the local effects of turbulence and stratification. Although the parameterizations of these functions presented here performed well for the test cases analyzed, they remain to be validated for more turbulent flows (i.e. higher  $Re_\tau$ ) and stronger stratification (i.e. higher  $Ri_\tau$ ). The models can only be improved by renewed theoretical reasoning and understanding of the physics of turbulent fluid dynamics in conjunction with additional field, laboratory, and DNS data to facilitate calibration and comparison. In addition to model parameter formulations, the discretization of the equations and meshing of the flow domain geometry can be improved in different ways using more accurate, higher order schemes and grid refinement to better capture the physics of the flow and

turbulence and reduce numerical errors. Other model parameters and constants (e.g.  $C_\mu$ ) may also need to be parameterized as functions of turbulence and stratification in order to achieve a more general model.

To this end, it is important to continue to obtain data for strongly stratified and inhomogeneous flows to facilitate ongoing efforts to develop better turbulence models for stably stratified flows. With the rapid advancement of computing power, memory, and speed, obtaining DNS data for higher Reynolds number flows and increasing geometric complexity needed to validate these models is becoming feasible. Overall, the best models are those that are universal in their description and broad in their application.

## REFERENCES

- Anderson, J.D. (1998). Some reflections on the history of fluid dynamics. In R.W. Johnson (Ed.), *Handbook of Fluid Dynamics* (pp. 2-1 – 2-15). Berlin: Springer.
- Armenio, V., & Sarkar, S. (2002). An investigation of stably stratified turbulent channel flow using large-eddy simulation. *J. Fluid Mech.*, 459, 1-42.
- Baum, E., & Caponi, E. (1992). Modeling the effects of buoyancy on the evolution of geophysical boundary layers. *J. Geophys. Res.*, 97, 15513-15527.
- Burchard, H., & Baumert, H. (1995). On the performance of a mixed-layer model based on the k- $\epsilon$  turbulence closure scheme. *J. Geophys. Res.*, 100, 8523-8540.
- Burchard, H., Bolding, K., & Villarreal, M.R. (1999). *GOTM – A General Ocean Turbulence Model. Theory, Applications and Test Cases*. European Commission Rep. EUR 18745 EN, 103 pp.
- Casulli, V., & Cattani, E. (1994). Stability, accuracy and efficiency of a semi-implicit method for three-dimensional shallow water flow. *Comput. Math. Appl.*, 27, 99-112.
- Chen, C., & Jaw, S. (1998). *Fundamentals of Turbulence Modeling*. New York: Taylor & Francis.
- Durbin, P.A., & Pettersson Reif, B.A. (2001). *Statistical Theory and Modeling for Turbulent Flows*. New York: Wiley.
- Fernando, H.J.S. (1991). Mixing efficiency in stratified shear flows. *Annu. Rev. Fluid Mech.*, 23, 455-493.
- Ferziger, J.H., & Peric, M. (2002). *Computational Methods for Fluid Dynamics*. Berlin: Springer.
- Fringer, O.B., Gerritsen, M., & Street, R.L. (2006). An unstructured-grid, finite-volume, nonhydrostatic, parallel coastal ocean simulator. *Ocean Modelling*, 14, 139-173.
- Galperin, B., Sukoriansky, S., & Anderson, P.S. (2007). On the critical Richardson number in stably stratified turbulence. *Atmos. Sci. Lett.*, 8, 65-69.

- García-Villalba, M., & del Álamo, J.C. (2009). Turbulence and internal waves in a stably-stratified channel flow. In Nagel, W.E., Kröner, D.B., & Resch, M.M (Eds.), *High Performance Computing in Science and Engineering '08* (pp. 217-227). Berlin: Springer.
- Gregg, M.C. (1987). Diapycnal mixing in the thermocline. *J. Geophys. Res.*, 92, 5249-5286.
- Ivey, G.N., Winters, K.B., & Koseff, J.R. (2008). Density stratification, turbulence, but how much mixing? *Annu. Rev. Fluid Mech.*, 40, 169-184.
- Jones, W.P., & Launder, B.E. (1972). The prediction of laminarization with a two-equation model. *Int. J. Heat Mass Transfer*, 24, 1541-1544.
- Kays, W.M. (1994). Turbulent Prandtl number. Where are we? *J. Heat Transfer*, 116, 284-295.
- Kays, W.M., & Crawford, M.E. (1993). *Convective Heat and Mass Transfer*. New York: McGraw-Hill.
- Kim, J., & Mahrt, L. (1992). Simple formulation of turbulent mixing in the stable free atmosphere and nocturnal boundary layer. *Tellus*, 44A, 381-394.
- Komori, S., Ueda, H., Ogino, F., & Mizushima, T. (1983). Turbulence structure in stably stratified open-channel flow. *J. Fluid Mech.*, 130, 13-26.
- Kundu, P.K. (1990). *Fluid Mechanics*. San Diego: Academic Press.
- Launder, B.E., & Spalding, D.B. (1972). *Mathematical Models of Turbulence*. London: Academic Press.
- Louis, J. (1979). A parametric model of vertical eddy fluxes in the atmosphere. *Boundary-Layer Meteorol.*, 17(2), 187-202.
- Louis, J., Tiedke, M., & Geleyn, J.F. (1981). A short history of the operational PBL-parameterization at ECMWF. *ECMWF Workshop on Planetary Boundary Layer Parameterization*, pp. 59-79.
- Moin, P., & Mahesh, K. (1998). Direct numerical simulation: a tool in turbulence research. *Annu. Rev. Fluid Mech.*, 30, 539-578.
- Moser, R.D., Kim, J., & Mansour, N.N. (1999). Direct numerical simulation of turbulent channel flow up to  $Re_\tau=590$ . *Phys. Fluids*, 11(4), 943-945.
- Munk, W.H., & Anderson, E.R. (1948). Notes on a theory of the thermocline. *J. Mar. Res.*, 7, 276-295.

- Peltier, W.R., & Caulfield, C.P. (2003). Mixing efficiency in stratified shear flows. *Annu. Rev. Fluid Mech.*, 35, 135-167.
- Peters, H., Gregg, M.C., & Toole, J.M. (1988). On the parameterization of equatorial turbulence. *J. Geophys. Res.*, 93, 1199-1218.
- Pope, S.B. (2000). *Turbulent Flows*. New York: Cambridge University Press.
- Riley, J.J., & Lelong, M.P. (2000). Fluid motions in the presence of strong stable stratification. *Annu. Rev. Fluid Mech.*, 32, 613-657.
- Rodi, W. (1993). *Turbulence Models and Their Application in Hydraulics*. Rotterdam: A.A. Balkema.
- Rodi, W. (1987). Examples of calculation methods for flow and mixing in stratified fluids. *J. Geophys. Res.*, 92, 5305-5328.
- Rogallo, R.S., & Moin, P. (1984). Numerical simulation of turbulent flows. *Annu. Rev. Fluid Mech.*, 16, 99-137.
- Shih, L.H., Koseff, J.R., Ferziger, J.H., & Rehmman, C.R. (2000). Scaling and parameterization of stratified homogeneous turbulent shear flow. *J. Fluid. Mech.*, 412, 1-20.
- Strang, E.J., & Fernando, H.J.S. (2001). Vertical mixing and transports through a stratified shear layer. *J. Phys. Oceanogr.*, 31, 2026-2048.
- Turner, J.S. (1973). *Buoyancy Effects in Fluids*. New York/London: Cambridge University Press.
- Umlauf, L., Burchard, H., & Bolding, K. (2007). *GOTM Sourcecode and Test Case Documentation*. Retrieved October 1, 2010, from <http://www.gotm.net>
- Venayagamoorthy, S.K., Koseff, J.R., Ferziger, J.H., & Shih, L.H. (2003). Testing of RANS turbulence models for stratified flows based on DNS data. *Center for Turbulence Research Annual Research Briefs*, pp. 127-138.
- Venayagamoorthy, S.K., & Stretch, D.D. (2006). Lagrangian mixing in decaying stably stratified turbulence. *J. Fluid Mech.*, 564, 197-226.
- Venayagamoorthy, S.K., & Stretch, D.D. (2010). On the turbulent Prandtl number in homogeneous stably stratified turbulence. *J. Fluid Mech.*, 644, 359-369.
- White, F.M. (1991). *Viscous Fluid Flow*. New York: McGraw-Hill.
- Wilcox, D.C. (1993). *Turbulence Modeling for CFD*. La Cañada: DCW Industries.

## **APPENDIX A**

### **MATLAB CODE FOR ZERO-EQUATION TURBULENCE MODEL**

#### **A.1 Introduction**

This appendix contains the MATLAB code developed to simulate and compute results for the zero-equation turbulence model study in section A.2. All coding and output of model results for chapter three were done in MATLAB.

## A.2 MATLAB Code for Zero-Equation Turbulence Model

```

%%%%%%%%%%%%%%%%%%%%%%%%%%%%%%%%%%%%%%%%%%%%%%%%%%%%%%%%%%%%%%%%%%%%%%%%
%
% Zach Elliott
% Colorado State University
% June 2010
%
% Code for one-dimensional fully developed stably stratified
% turbulent channel flow to test vertical turbulent mixing with
% zero-equation turbulence model
%
%%%%%%%%%%%%%%%%%%%%%%%%%%%%%%%%%%%%%%%%%%%%%%%%%%%%%%%%%%%%%%%%%%%%%%%%

clear;
clf;

%Define parameters (SI units)
theta=0.7;
H=15;
N=81;
dz=H/(N-1);
U_max=0.75;
T=21600*2; %(i.e. 12 hour M2 tidal period)
g=9.81;
rho_0=1000;
drho=30;
beta=10;
alpha=-1/2;
beta_rho=10/3;
alpha_rho=-3/2;
z_1=-8; %upper stratified layer depth
z_2=-12; %lower stratified layer depth
z_mid=(z_1+z_2)/2; %middle of stratified layer
nu=1e-06;
epsilon=1e-05; %prevents Richardson number from going to infinity
Pr_t0=0.7; %neutral turbulent Prandtl number
gamma_inf=1/3; %mixing efficiency
Ri_inf=1/4; %flux Richardson number
kappa=0.41;
z_b=2; %ratio of z_b/z_0 for bed roughness assuming log velocity profile
C_D=((1/kappa)*log(z_b))^2;
dC=10; %concentration in ppt
z_1C=-9; %upper concentration boundary depth
z_2C=-15; %lower concentration boundary depth
M=10700;
dt=55;
s=dt/(2*dz^2); %Diffusion Courant number
fname='/home/zach/Movies/movie'; %Directory for storing movie images

%Define grid points z(i)
for i=1:N;
    z(i)=-H+dz*(i-1);
end

%Define initial parameter distributions

%Density stratification profile (continuous)
%for i=1:N;
%    rho(i)=rho_0-(drho*z(i))/H;
%end

%Density stratification profile (two-layer)
for i=1:N;
    if z(i)<=z_2
        rho(i)=rho_0+drho;
    elseif z(i)<=z_1
        rho(i)=rho_0+(1/2)*drho*(1+cos(pi*(z(i)-z_2)/(z_1-z_2)));
    else
        rho(i)=rho_0;
    end
end

%Plot density stratification profile
figure(1);
plot(rho,z);

```

```

        title('Density Stratification Profile','FontSize',16)
        xlabel('\rho (kg/m^3)','FontSize',12)
        ylabel('z (m)','FontSize',12)
        axis([rho_0-2*drho rho_0+3*drho -H 0])
        grid on

%Brunt-Vaisala frequency distribution
N_BV(1)=0;
N_BV(N)=0;
for i=2:N-1;
    N_BV(i)=sqrt((-g/rho_0)*(rho(i+1)-rho(i-1))/(2*dz));
end

%Concentration profile
for i=1:N;
    if z(i)<=z_2C
        C(i,1)=0;
    elseif z(i)<=z_1C
        C(i,1)=-dc*(sin(pi*(z(i)-z_2C)/(z_2C-z_1C)));
    else
        C(i,1)=0;
    end
end

%Plot initial concentration profile
figure(2);
plot(C(:,1),z);
title('Initial Concentration Profile','FontSize',16)
xlabel('C (ppt)','FontSize',12)
ylabel('z (m)','FontSize',12)
axis([0 dc -H 0])
grid on

%Define explicit coefficient tridiagonal matrices
b1=zeros(size(1:N-1));
b2=-1.*ones(size(1:N));
b3=ones(size(1:N-1));
B=diag(b1,-1)+diag(b2,0)+diag(b3,1);
B(N,N-1)=1;
d1=-1.*ones(size(1:N-1));
d2=ones(size(1:N));
d3=zeros(size(1:N-1));
D=diag(d1,-1)+diag(d2,0)+diag(d3,1);
D(1,2)=-1;

%Define eddy viscosity tridiagonal matrices N_plus and N_minus
n_plus_1=zeros(size(1:N-1));
n_plus_2=ones(size(1:N));
n_plus_3=ones(size(1:N-1));
N_plus=diag(n_plus_1,-1)+diag(n_plus_2,0)+diag(n_plus_3,1);
n_minus_1=ones(size(1:N-1));
n_minus_2=ones(size(1:N));
n_minus_3=zeros(size(1:N-1));
N_minus=diag(n_minus_1,-1)+diag(n_minus_2,0)+diag(n_minus_3,1);

%Initialize velocity field for uni-directional flow
%load u_CF_developed
%u=u_CF_developed;

%Initialize velocity field for oscillatory flow
u(1:N,1) = zeros(N,1);

%Time loop to march forward in time based on selected time step dt
for n=1:M;

    %Update current time
    t(n)=dt*(n-1);

    %Compute gradient Richardson number distribution
    Ri(1)=0;
    Ri(N)=0;
    for i=2:N-1;
        Ri(i)=(N_BV(i))^2/(epsilon+((u(i+1,n)-u(i-1,n))/(2*dz))^2);
    end

    %Compute "factor(i)"=(1+beta*Ri(i))^alpha
    for i=1:N;
        factor(i)=(1+beta*Ri(i))^alpha;
    end

    %Compute "factor_rho(i)"=(1+beta_rho*Ri(i))^alpha_rho

```

```

        for i=1:N;
            factor_rho(i)=(1+beta_rho*Ri(i))^alpha_rho;
        end

%Compute turbulent Prandtl number distribution (Munk and Anderson 1948)
%for i=1:N;
%    Pr_t(i)=Pr_t_0*factor(i)/factor_rho(i);
%end

%Compute turbulent Prandtl number distribution (Venayagamoorthy and Stretch 2010)
for i=1:N;
    Pr_t(i)=Pr_t_0*exp(-Ri(i)/(Pr_t_0*gamma_inf))+(Ri(i)/Ri_inf);
end

%Compute turbulent Prandtl number distribution (Kim and Mahrt 1992)
%for i=1:N;
%    Pr_t(i)=Pr_t_0*(1+15*Ri(i)*(1+5*Ri(i))^(1/2))/(1+10*Ri(i)*(1+5*Ri(i))^(1/2));
%end

%Compute turbulent Prandtl number distribution (Peters et al. 1988)
%for i=1:N;
%    if Ri(i)==0
%        Pr_t(i)=Pr_t_0;
%    elseif Ri(i)<=0.25
%        Pr_t(i)=(56/3)*Ri(i)^1.4;
%    else
%        Pr_t(i)=(5*(1+5*Ri(i))^-1.5+0.2)/(5*(1+5*Ri(i))^-2.5+0.01);
%    end
%end

%Compute bed shear velocity u_star
u_star=sqrt(C_D)*u(1,n);

%Compute eddy viscosity profile vector nu_t (no cut-off)
%for i=1:N;
%    nu_t(i)=nu+factor(i)*kappa*abs(u_star)*(-z(i)/H)*(H+z(i));
%end

%Compute eddy viscosity profile vector nu_t (cut-off)
for i=1:N;
    i_mid=round((z_mid+H)/dz);

    if z(i)<=z(i_2)
        nu_t(i)=nu+factor(i)*kappa*abs(u_star)*(-z(i)/H)*(H+z(i));
    else
        nu_t(i)=nu+factor(i_mid)*kappa*abs(u_star)*(-z(i_mid)/H)*(H+z(i_mid))
            *(z(i)/z(i_mid))*(2-(z(i)/z(i_mid)));
    end
end

%Compute eddy diffusivity profile vector gamma_t
for i=1:N;
    gamma_t(i)=nu_t(i)./Pr_t(i);
end

%Compute spatially averaged eddy viscosity terms vector
nu_t_plus=N_plus*nu_t';
nu_t_minus=N_minus*nu_t';

%Compute spatially averaged eddy diffusivity terms vector
gamma_t_plus=N_plus*gamma_t';
gamma_t_minus=N_minus*gamma_t';

%Compute velocity boundary condition matrix E
E=zeros(N,1);
E(1,1)=-2*s*(1-theta)*nu_t_minus(1)*dz*(C_D/nu_t(1))*abs(u(1,n))*u(1,n);

%Update explicit coefficient tridiagonal matrices with eddy viscosity and eddy
diffusivity
for i=1:N
    B_u(i,:)=(nu_t_plus(i)).*B(i,:);
    D_u(i,:)=(nu_t_minus(i)).*D(i,:);
    B_C(i,:)=(gamma_t_plus(i)).*B(i,:);
    D_C(i,:)=(gamma_t_minus(i)).*D(i,:);
end

%Define implicit tridiagonal velocity coefficient matrix A
a=(s*theta).*nu_t_plus;
b=(s*theta).*nu_t_minus;
c=1+a+b;

```

```

A=diag(-1*a(1:N-1),1)+diag(c(1:N),0)+diag(-1*b(2:N),-1);
A(1,2)=-b(1)-a(1);
A(1,1)=c(1)+2*b(1)*dz*(C_D/nu_t(1))*abs(u(1,n));
A(N,N-1)=-b(N)-a(N);

%Matrix equation to solve for u(:,n+1)
u(:,n+1)=A\u(:,n)+U_max*dt*(2*pi/T)*cos(2*pi*t(n)/T)+(s*(1-theta)).*B_u*u(:,n)
-(s*(1-theta)).*D_u*u(:,n)+E);

%Plot velocity field at current time step n u(:,n)
figure(3);
plot(u(:,n),z);
title('velocity Profile','FontSize',16)
xlabel('u (m/s)','FontSize',12)
ylabel('z (m)','FontSize',12)
axis([-1 1 -H 0])
grid on
pause(0.1)

%This part of the loop outputs .jpg images at every time step in directory fname
if (n<10)
    str=['000',num2str(n)];
elseif (n>9 && n<100)
    str=['00',num2str(n)];
elseif (n>99 && n<1000)
    str=['0',num2str(n)];
else
    str=num2str(n);
end
scale=100;
P(n)=getframe;
eval(['print -djpeg ',fname,str]);
unix(['convert','',fname,str,'.jpg ',' ',fname,str,'.gif']);

%Define implicit tridiagonal concentration coefficient matrix A_C
a_C=(s*theta).*gamma_t_plus;
b_C=(s*theta).*gamma_t_minus;
c_C=1+a_C+b_C;

A_C=diag(-1*a_C(1:N-1),1)+diag(c_C(1:N),0)+diag(-1*b_C(2:N),-1);
A_C(1,2)=-b_C(1)-a_C(1);
A_C(N,N-1)=-b_C(N)-a_C(N);

%Matrix equation to solve for C(:,n+1)
C(:,n+1)=A_C\C(:,n)+(s*(1-theta)).*B_C*C(:,n)-(s*(1-theta)).*D_C*C(:,n));

%Plot concentration field at current times step n C(:,n)
figure(4);
plot(nu_t(:,z));
title('Concentration Distribution','FontSize',16)
xlabel('C (ppt)','FontSize',12)
ylabel('z (m)','FontSize',12)
axis([0 0.05 -H 0])
grid on
pause(0.1)

%This part of the loop outputs .jpg images at every time step in directory fname
if (n<10)
    str=['000',num2str(n)];
elseif (n>9 && n<100)
    str=['00',num2str(n)];
elseif (n>99 && n<1000)
    str=['0',num2str(n)];
else
    str=num2str(n);
end
scale=100;
P(n)=getframe;
eval(['print -djpeg ',fname,str]);
unix(['convert','',fname,str,'.jpg ',' ',fname,str,'.gif']);
end

```

## APPENDIX B

### FORTRAN95 CODE FOR MODIFIED GOTM MODULES

#### B.1 Introduction

This appendix provides the FORTRAN95 code for each of the GOTM modules or subroutines that were modified or created to simulate and compute results using the  $k$ - $\varepsilon$  model pertaining to the study in chapter four. Section B.2 contains the GOTM module buoyancy.F90 that was modified to set Dirichlet boundary conditions in the channel to impose stratification on the flow after it had fully developed. Section B.3 gives the subroutine cmue\_vs.F90 that was created to define the stability function for the  $k$ - $\varepsilon$  model according to the Venayagamoorth and Stretch (2010) formulation of  $Pr_t$  and section B.4 gives the subroutine cmue\_frk.F90 that was created to implement the stability functions for  $Pr_t$  and  $C_{\varepsilon 3}$  as functions of  $Fr_k$  in the  $k$ - $\varepsilon$  model in GOTM.

## B.2 buoyancy.F90 GOTM Module

```

-----
!BOP
!
!ROUTINE: The buoyancy equation
!
!INTERFACE:
  subroutine buoyancy(nlev,dt,cnpar,nuh,n)
!
!DESCRIPTION:
  This subroutine computes the transport of the buoyancy,
  \begin{equation}
  \label{DefBuoyancy}
  b=-g\frac{\rho-\rho_0}{\rho_0}
  \end{equation}
  where $g$ is the acceleration of gravity, and $\rho$ and $\rho_0$
  are the actual and the reference density.
  A simplified transport equation for $b$ can be written as
  \begin{equation}
  \label{bEq}
  \dot{b}
  = {\cal D}_b
  \end{equation}
  where $\dot{b}$ denotes the material derivative of $b$, and
  ${\cal D}_b$ is the sum of the turbulent and viscous transport
  terms modelled according to
  \begin{equation}
  \label{Db}
  {\cal D}_b
  = \text{frstder}\{z\}
  \left(
  \nu'_t \text{partder}\{b\}\{z\}
  \right)
  \text{point}
  \end{equation}
  In this equation, $\nu'_t$ is the turbulent diffusivity
  of buoyancy.
  The computation
  of $\nu'_t$ is discussed in \sect{sec:turbulenceIntro}. Note,
  that the model \eq{DS} assumes that turbulent transport of heat
  and salt is identical. Source and sink
  terms are completely disregarded, and thus \eq{bEq} serves
  mainly as a convenient tool for some idealised test cases in
  GOTM.

  Diffusion is treated implicitly in space (see equations (\ref{sigmafirst})-
  (\ref{sigmalast})), and then solved by a
  simplified Gauss elimination.
  Vertical advection is included for accounting for adaptive grids,
  see \tt adaptivegrid.F90}.
!
!USES:
  use mtridiagonal
  use meanflow,    only:  h,ho,buoy,avh,w,w_grid,grid_method
  use observations, ONLY:  b_obs_NN,b_obs_surf,b_obs_sbf
  use observations, ONLY:  w_adv_discr,w_adv_method
!
  IMPLICIT NONE
!
!INPUT PARAMETERS:
  integer, intent(in)           :: nlev,n
  double precision, intent(in)  :: dt,cnpar
  double precision, intent(in)  :: nuh(0:nlev)
!
!REVISION HISTORY:
  Original author(s): Hans Burchard & Karsten Bolding
!
  $Log: buoyancy.F90,v $
  Revision 1.5  2003/03/28 09:20:35  kbk
  added new copyright to files
!
  Revision 1.4  2003/03/28 08:56:56  kbk
  removed tabs
!

```

```

!
! Revision 1.3 2003/03/10 08:50:06 gotm
! Improved documentation and cleaned up code
!
! Revision 1.1.1.1 2001/02/12 15:55:57 gotm
! initial import into CVS
!
!EOP
!
! LOCAL VARIABLES:
integer                :: i,Meth,Bcup,Bcdw,flag
double precision       :: zz,tot
logical, save         :: first=.false.
double precision       :: Qsour(0:nlev),RelaxT(0:nlev)
double precision       :: Tup,Tdw,z
logical               :: surf_flux,bott_flux
!
!-----
!BOC
! Construct initial linear profile from information in namelist
!print*,'n=',n
! Imposing stratification after flow develops
if( n .eq. 88200)then
first=.true.
endif

if (first) then
zz=0.0
do i=nlev,1,-1
zz=zz+0.5*h(i)
buoy(i) = b_obs_surf - zz*b_obs_NN
zz=zz+0.5*h(i)
!print*,'h=',h(i),zz,buoy(i)
end do
first=.false.
else
buoy(i)=0.
end if

! Set Dirichlet boundary conditions
Bcup=2                !BC Dirichlet
Tup=b_obs_sbf         !Buoyancy flux
Bcdw=2                !BC Dirichlet
if(n .ge. 88200) then
Tdw=-0.0038341875
else
Tdw=0.
endif                  !No flux
surf_flux=.false.
bott_flux=.false.

avh=nuh
Qsour=0.
RelaxT=1.e15

flag=1 ! divergence correction for vertical advection

call Yevol(nlev,Bcup,Bcdw,dt,cnpar,Tup,Tdw,RelaxT,h,ho,avh,w, &
Qsour,buoy,w_adv_method,w_adv_discr,buoy,surf_flux, &
bott_flux,grid_method,w_grid,flag)

return
end subroutine buoyancy
!EOC
!
!-----
! Copyright by the GOTM-team under the GNU Public License - www.gnu.org
!-----

```

### B.3 cmue\_vs.F90 GOTM Module

```
!-----  
!BOP  
! 12/1/10 for GOTM v. 3.0  
! ROUTINE: Venayagamoorthy and Stretch (2010) stability function  
!  
!   subroutine cmue_vs(nlev)  
!  
! DESCRIPTION:  
! This subroutine computes stability functions according to the  
! Venayagamoorthy and Stretch (2010) model for Pr_t based on simulation  
! data on stratified homogeneous shear-flows:  
!  
!       Turbulent Prandtl number  
!       Pr_t = Pr_t0*exp(-Ri/(Pr_t0*Gamma_inf))+Ri/Ri_inf  
!  
! where Pr_t0 is the neutral value of Ri Pr_t, Ri is the gradient  
! Richardson number, Gamma_inf is the mixing efficiency, and Ri_inf is  
! the flux Richardson number.  
!  
! USES:  
! use turbulence, only: Prandtl0_fix,cm0_fix  
! use turbulence, only: cmue1,cmue2,as,an  
! IMPLICIT NONE  
!  
! INPUT PARAMETERS:  
! integer, intent(in)           :: nlev  
!  
!EOP  
!  
! LOCAL VARIABLES:  
! integer                :: i  
! double precision      :: Ri,Prandtl  
!  
!-----  
!BOC  
! do i=1,nlev-1  
!   Ri=an(i)/(as(i)+1.e-8) ! Gradient Richardson number  
!   if (Ri.ge.1e-10) then  
!     Prandtl=Prandtl0_fix*exp(-Ri/(Prandtl0_fix*(1/3)))+Ri/0.25  
!   else  
!     Prandtl=Prandtl0_fix  
!   end if  
!  
!   cmue1(i)=cm0_fix  
!   cmue2(i)=cm0_fix/Prandtl  
!  
! end do  
! return  
! end subroutine cmue_vs  
!EOC  
!-----
```

## B.4 cmue\_frk.F90 GOTM Module

```

-----
!BOP
! 12/8/10 for GOTM v. 3.0
! ROUTINE: Stability function for Pr_t and C_eps3 as functions of Fr_k
!
!   subroutine cmue_frk(nlev, n, dt)
!
! DESCRIPTION:
! This model modifies the coefficients of the k-eps turbulence model
! to vary with depth (and stratification):
!
!   Turbulent Prandtl number
!   Pr_t = 3*exp(0.1*Fr_k)+Pr_t0
!         this is Prandtl0 in the turbulence module
!
!   C_eps3 = C_eps30*exp(-Fr_k)
!         this is ce3minus in the turbulence module
!         note: this model is for stable stratification only a value for
!               ce3minus is specified. ce3plus is for unstable
!               stratification retains its default value.
!
! Compute Fr_k as
!   Fr_k = eps/Nk
! and
!   epsilon = dissipation = eps, in turbulence module
!   N = buoyancy frequency = NN in meanflow module
!   k = TKE = tke in turbulence module
!   nu = molecular viscosity = avmolu in meanflow module
!   P = production = P in meanflow module
!
! USES:
! use turbulence, only: eps, tke
! use turbulence, only: ce1, ce2, ce3minus, sig_k, cmue1, cmue2
! use turbulence, only: ce2_0, ce3minus_0, sig_k0
! use turbulence, only: cm0_fix, Prandtl0_fix
! use meanflow, only: NN, avmolu, P
! implicit none
!
! INPUT PARAMETERS:
! integer, intent(in) :: nlev
! integer, intent(in) :: n
! double precision, intent(in) :: dt
!
! LOCAL VARIABLES
! double precision :: Fr_k, Prandtl
! integer :: i
! double precision :: old_ce2, old_ce3minus, old_cmue1, old_sigk
! double precision :: eddy_turn
!
!
! EOP
-----
! BOC
! Set the coefficients to the standard k-eps values for the first time step
! open(21, file='parameters.dat', status='unknown', form='formatted')
! if( n .ge. 88200 ) then
!
! approx. one eddy turnover time
!   eddy_turn = sum(eps)/sum(tke)
!
!   do i=1,nlev-1
! save the last values of the variables for the first eddy-turnover time
!
!   if( n*dt .lt. eddy_turn) then
!     old_ce2 = ce2(i)
!     old_ce3minus = ce3minus(i)
!     old_cmue1 = cmue1(i)
!     old_sigk = sig_k(i)
!   endif
!
! calculate parameters relating to turbulence for this grid point
!   !Fr_k = eps(i)/sqrt(NN(i))/tke(i)

```

```

! calculate parameters relating to stratification for this grid point
      if( NN(i) .gt. 1e-8 ) then
        Fr_k = eps(i)/sqrt(NN(i))/tke(i)
! update the values for the coefficients Pr_t and C_eps3
        Prandt1=2.0*exp(-0.1*Fr_k)+Prandt10_fix
        ce3minus(i) = 0.48*exp(-Fr_k)
        else ! default to standard k-eps for NN(i) = 0
! in the unstratified limit, the model reverts to the standard k-eps model
        ce2 = ce2_0
        ce3minus(i) = ce3minus_0
        Prandt1 = Prandt10_fix
        cmue1(i)=cm0_fix
        endif

      enddo ! end of vertical grid loop

    else ! default to standard k-eps for first time step

      ce2 = ce2_0
      ce3minus = ce3minus_0
      Prandt1 = Prandt10_fix
      cmue1=cm0_fix
      cmue2=cm0_fix/Prandt1

    endif

    return
  end subroutine cmue_frk
! EOC
!-----

```